Construction and Building Materials 266 (2021) 121009

Contents lists available at ScienceDirect

Construction and Building Materials

journal homepage: www.elsevier.com/locate/conbuildmat

Accelerate ageing on building stone materials by simulating daily, seasonal thermo-hygrometric conditions and solar radiation of Csa Mediterranean climate

Fabio Sitzia [a,b,*], Carla Lisci [a,b], José Mirão [a,b]

[a] HERCULES Laboratory, Institute for Advanced Studies and Research, University of Évora, Largo Marquês de Marialva 8, 7000-809 Évora, Portugal
[b] Geosciences Department, School of Sciences and Technology, University of Évora, Rua Romão Ramalho 59, 7000-671 Évora, Portugal

HIGHLIGHTS

- Water salinity degree is crucial in stone physical decay.
- Stone colour changing is due to the oxidation of organic matter and iron.
- Ageing on geo-materials causes a general decrease of mechanical proprieties.
- Natural outdoor weathering must verify accelerated testing.

ARTICLE INFO

Article history:
Received 17 May 2020
Received in revised form 15 August 2020
Accepted 15 September 2020

Keywords:
Accelerate ageing
Photogrammetry
Weathering
Solar radiation
Temperature
Relative humidity
Capillary rising

ABSTRACT

The maintenance plan of ancient and contemporary buildings today takes on strategic importance and should include the identification of climatic environment where the structures are located. Researcher are trying to evaluate the response to weathering of the building materials by accelerated ageing tests. This technique often consists of the "aggravations practice", by subjecting materials to extreme climate parameters not representative of the real environment conditions. For this reason, this type of ageing presents a lot of criticisms. This research addresses the lacking of literature about the realistic simulation of a determinate environment/climate on building stone materials. The aim of this research is to understand if it is possible to recreate in laboratory the pathologies observed on building stones of ancient monuments from Sardinia (Italy) by simulating the climatic context of location. To do so, samples were undergone to accelerated cycles of thermo-hygrometric conditions and solar radiation for simulating realistic parameters of Csa Mediterranean climate. Monitoring of some physical/mechanical properties before and after ageing indicates an overall decohesion of samples, the appearance of decay patinas and a slight worsening of mechanical resistances. A mathematical equation relates the ageing test duration (6 months) with the hypothetical outdoor exposure quantifiable in ≈18 years for samples evolved to temperature and humidity cycles while ≈3.7 years for the samples subjected to only solar radiation. However, the test should to be reproduced in the natural outdoor environment to correlate and verify the reliability of the obtained data (test the test).

1. Introduction

The response of natural and artificial building materials to weathering is important for civil engineering, architecture and research especially for an accurate conservation of contemporary great works and Cultural Heritage. For this reason, the scientific community is today trying to evaluate and predict this response in laboratory by subjecting building materials to accelerated environmental stresses (ageing).

Ageing is an experimental technique that accelerated the normal decay processes by using aggravated conditions or rapid cycles of temperature, relative humidity, O_2, CO, CO_2, SO_X, NO_X air concentration and UV radiations on a wide typology of materials (e.g. building stones, concretes, paints, wood, plastic coats, automotive components, geotextile) [1–5].

A common criticism about ageing indicates that the decay caused by aggravated conditions of temperature, relative humidity,

* Corresponding author at: 1a Italy street, Decimomannu, Cagliari Post code: 09033, Italy.
E-mail address: fasitzia@tiscali.it (F. Sitzia).

https://doi.org/10.1016/j.conbuildmat.2020.121009
0950-0618/

solar radiation and other parameters in the short term, is different from the natural decay in long term [6]. Accelerated ageing and natural ageing processes are, therefore, not parallel and accelerate ageing data must be compared with a real outdoor weathering data (practice of "test the test"). Normally, has been detected that artificial cyclic exposures tend to be more severe than natural exposures [7].

Too much reliance only on accelerated testing can be potentially misleading [7], for this reason some researchers have begun to compare materials undergone to accelerated ageing with materials undergone to natural ageing [8].

On building stone materials, ageing tests are mainly used to examine the basic processes of decay according to international standards consisting of aggravating parameter practice [9–12].

For example, freeze–thaw ageing (F-T, ASTM D5312:2013 [13]) consists of submitting stone samples to controlled freezing and thawing conditions (−20 °C, 20 °C). This technique has been used by some authors [14–16] who have detected a loss of weight of the samples due to the decohesion, and an overall reduction of mechanical features (e.g. compressive wave velocity, uniaxial compressive strength). A general decrease of open porosity has been recorded in the samples subjected to F-T cycles [14]. In the same work both decrease and increase of partial porosity relative to pore size ranges of < 0.1, 0.1–1, 1–10, 10–100, >100 μm have been detected.

Heating-cooling ageing (H-C) according to UNI EN 14066:2013 [17], submits stone samples to aggravated heating (105 °C) and cooling (20 °C) conditions. According to some authors [18–20], H-C ageing on stone sample materials causes a loss weight for decohesion, a decrease of compressive wave velocity, uniaxial compressive strength and point load index and modifications of stone colour and gloss. Multuturk et al. [10] indicated how H-C and F-T ageing on limestones, marbles and diabases cause a slight but constant decreases of hardness in terms of Shore scale (SH).

Besides H-C, F-T ageing, H-C-W (a combination of heating–cooling with total immersion) is also considered an aggravated ageing practice. It is possible to consider as ageing test also the saline crystallization experiment (UNI EN 12370:2001 [21]). The test determines the resistance to salt crystallisation of stone materials by using a 14% solution of Na_2SO_4 and a drying environment at 105 °C temperature. Saline crystallization on building stone materials according to the normative have been investigated by some authors. The acid solutions used in normative cause the stones weathering strongly dependent on their pore framework and textural characteristics [22]. In addition, UNI EN 12370 test also produces spalling, radial and crumbling deteriorations of stones [9], moderate open porosity increases [23] and an increase of mineral surface roughness [24]. This last author also show how the natural physical weathering of stones is accelerated by the internal crystallization pressure and increasing of the intra-granular and inter-granular micro fractures on feldspar crystals and the opening of cleavage planes of phyllosilicates.

Other types of ageing test include the determination of resistance to SO_2 action in presence of humidity as indicates by the normative UNI EN 13919:2004 [25]. This technique consists of the reproduction of a strongly SO_2 acid atmosphere given by the evaporation of a H_2SO_3 solution on moisture climatic chamber. Gibeaux et al. [26] have used this test in order to simulate the acid weathering on natural and artificial building stones according to the current atmospheric SO_2/NO_x rate. It has also been shown how the reaction between sulphur dioxide and limestones produces the formation of gypsum crust together with the change in the surface colour of the stone [27].

Other authors used the UNI EN 13919:2004 normative to test siloxane-based polymers coatings on limestones [28].

Other normative as the DIN 50018:1997 (Kesternich test) [29], born for evaluating the SO_2 corrosion testing in a saturated atmosphere on metals, is sometimes used on building materials [23]. Kesternich test realized on brick materials conducted to the formation of gypsum crystals in a very short period of time (24 h) [30]. The same authors show that during the test, sulfuric acid attacks Ca-rich high-temperature silicates such as wollastonite, gehlenite and Ca-feldspars, resulting in the formation of gypsum crystals.

The above-mentioned ageing tests consist of the reproduction of environments that do not reflect real natural conditions due to extreme complexity of natural outdoor, difficult to simulate in the laboratory. The new task of accelerated ageing is trying to simulate the real environmental conditions instead of aggravating weather imposed by the normative.

A lack of research about full ageing simulation of the climatic-environmental contexts occur. However, some authors [31] in the field of geo-materials, have ultimately realized partially methodical test where cement and mortar samples were subjected to a number of F-T cycles according to ASTM D5312 standard, but using the average max. and min. temperatures of a determinate place (Northern Portugal), instead of + 20 °C and −20 °C required by the standard.

These authors demonstrated, by measuring the loss weight, how pozzolanic mortars showed a better behaviour to ageing especially when compared to pure lime mortars.

In another paper focused on durability of lime-based mortars [32], authors try to reproduce extreme but real temperature, relative humidity and Na_2SO_4 aerosol deposition typical of a polluted city located in Southern Spain.

The following research address the above-mentioned lacking of literature about the full realistic simulation of a determinate environment/climate. Starting from *in situ* observations on ancient monuments of Sardinia (Italy), authors identified a wide range of building materials pathologies (e.g. granular decohesion, alveolization, efflorescences, detachments), some of which were particularly extensive so that compromise the structural safety of the buildings.

For this reason, the research questions were: i) is it possible to recreate in laboratory all the observed building materials pathologies by simulating the environment and the climatic context where the buildings are located? and ii) is this simulation reliable and predictive?

According to Köppen classification [33], Sardinia is mainly affected by hot-summer Mediterranean climate (Csa). This is characterised by a long period of summer drought and rainy winters with mild temperatures. In Europe, Mediterranean Sea is a fundamental regulator of climate and it is considered the transition zone between tropical areas, where seasons are defined according to the rainfall amount, and temperate zones, where seasons are characterised by clear temperature variations [34,35].

Csa climate not only affects Mediterranean basin but, at similar North and South latitudes ($25 < \varphi < 45°$), is present in Western United States, Latin America, Southern Africa and South-western Australia (Fig. 1a).

Globally, places engaged by Csa show an average annual temperature $15 < T_{Average} < 20$ °C with mean annual precipitation $200 < R_{Average} < 1200$ mm [36,37]. In this climatic context, building stone materials suffer from very slight weathering (VSW) to moderate chemical weathering (MCW) [38].

To fully reproduce the real conditions of Csa Mediterranean climate, the same stone samples of monuments construction were subjected to accelerated daily and seasonal cycles of temperature and humidity in a CO_2-bearing atmosphere with the help of a FITOCLIMA climatic chamber set according to meteorological Sardinian databases.

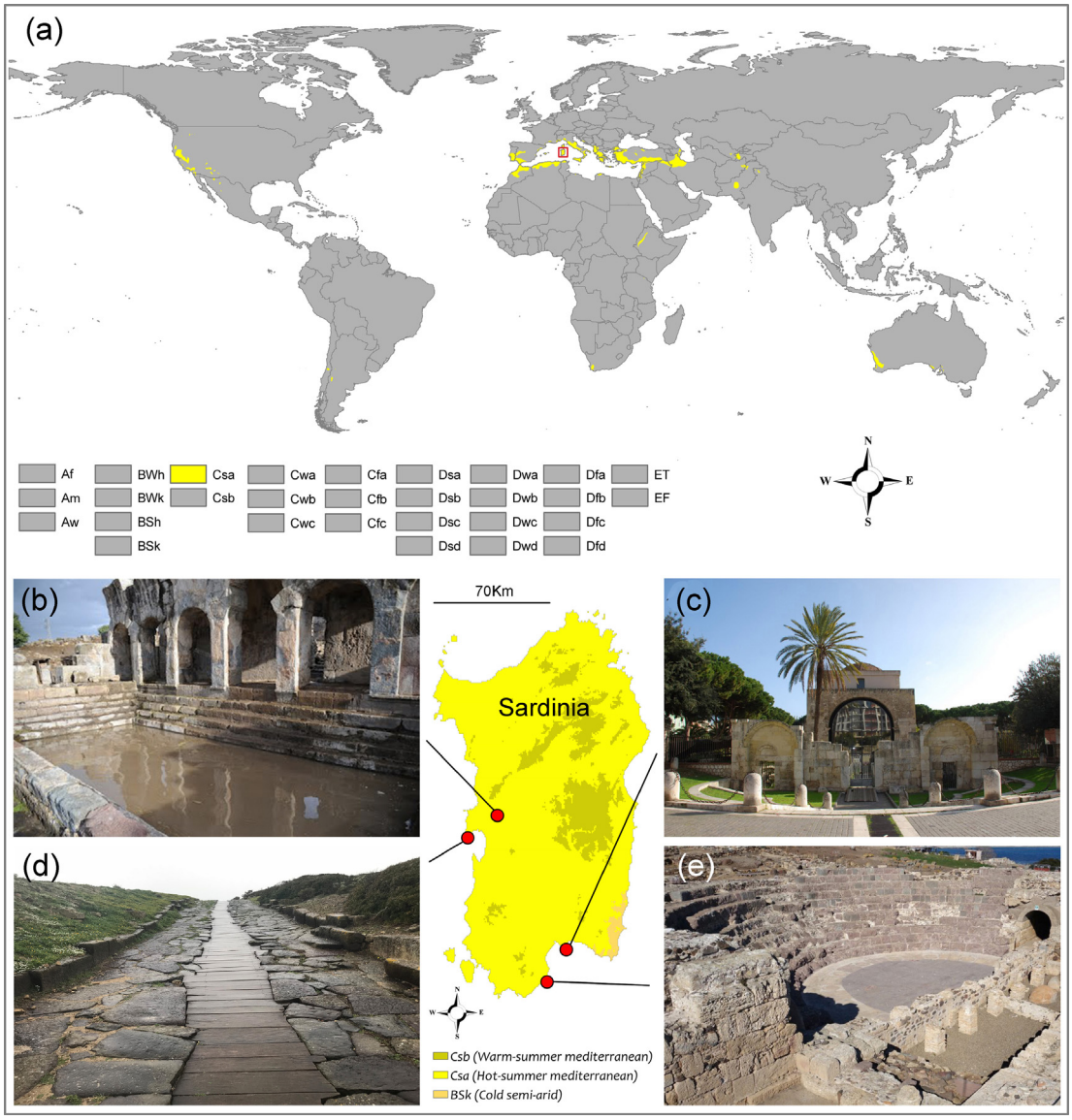

Fig. 1. (a) world distribution of hot-summer Csa Mediterranean climate [1], (b) thermal baths of *Forum Traiani*, (c) San Saturnino Basilica, (d) *Cardo Maximus* paving of *Tharros* archaeological area, (e) *Nora* Theatre (from: http://nora.beniculturali.unipd.it/gli-edifici/edifici-pubblici/teatro/).

A SOLARBOX climatic chamber set according to meteorological Sardinian databases was used for reproducing only the solar irradiation on the stones.

The novelties of this work are also given by:

I. crystallization tests not conducted using standard solution according to normative (14% vol. Na_2SO_4), but rather with *in situ* collected saline water (e.g. groundwater, seawater and thermal water) and rainwater;
II. monitoring the morphological and geometric variations of the sample by 3D micro-photogrammetry models (free available online) instead of ordinary photos;
III. image analysis of particle-size distribution of decohesion residue;
IV. the introduction of the new concept "hypothetical outdoor exposure" absent on literature;

Starting from those case studies at regional scale, this type of full simulation accelerate ageing can be used as a potential research protocol for assessing the decay resistance on dimension stones [39,40]. Ageing test realized with this protocol could be also conducted as strategic evaluation response of mortar, concrete, wall painting, brick, tile, wood, composite, paving that are intend to be used in specific climatic contexts [41–44]. Nowadays, those tests on climatic chamber are also mandatory to evaluate the long-term performance assessment of advance coatings and protective [45,46], consolidants [47,48] and other repair materials [49,50].

2. Materials and methods

2.1. Materials

In order to reproduce the decay of building stone materials, some lithologies (e.g. Thyrrenian Sandstone, biomicrite, biolitite, basalt, Carrara marble, rhyodacite, and two chromatic *facies* rhyolites) used in the construction of four most important historical monuments of Sardinia were selected (Table 1). Some of these lithologies also are used outside Italy and some others are used

Table 1
Case study monuments (Sardinia, Italy).

Case study monuments	Location	Age	Architectural style	Stone building material
Forum Traiani Baths	Fordongianus	I-IV cent. AD	Roman	Rhyolite (red and green *facies*)
San Saturnino Basilica	Cagliari	IV-XII cent. AD	Roman, Romanesque	Carrara marble, biomicrite, biolitite
Tharros buildings	Cabras	II cent. AD	Roman	Basalt, sandstone
Nora Theatre	Pula	III cent. AD	Roman, Phoenician-Punic	Rhyodacite

both in historic and contemporary architecture all around the world due to their technical and aesthetical qualities [51–57].

To carry out the tests, above-mentioned stones were collected into quarries identified by bibliography and cross geochemical-petrographic and isotopic comparisons between stone monument and outcrops materials [58–60].

The case study monuments (Table 1) are represented by *Forum Traiani* baths (Fig. 1b), San Saturnino Basilica (Fig. 1c), buildings of *Tharros* archaeological area (e.g. *Domus*, *pavings*, Fig. 1d) and *Nora* Theatre (Fig. 1e).

By FITOCLIMA climatic chamber, to fully reproduce the weather conditions affecting the monuments, samples underwent daily and seasonal cycles of temperature and relative humidity in a CO_2 air concentration.

Samples placed on FITOCLIMA chamber present two different dimensions:

$50 \times 50 \times 50$ mm ± 5 mm
$15 \times 15 \times 15$ mm ± 2 mm

Those two specimens size are necessary because some physical properties (e.g. density, imbibition coefficient, point load strength) are better measured on $15 \times 15 \times 15$ mm ± 2 mm specimens. Other monitored proprieties (e.g. mass, 3D morphologic characteristics) are better evaluable on 50x50x50mm ± 5 mm specimens.

In FITOCLIMA chamber, samples are organized in 2 sets for every lithology (Table 2). A set consist in 6 samples:

- one sample $50 \times 50 \times 50$ mm ± 5 mm dimension
- five samples $15 \times 15 \times 15$ mm ± 2 mm dimension

As in Table 2, for example, the first set of basalt consists of BA1 sample (dimension $50 \times 50 \times 50$ mm ± 5 mm) and BA1a, BA1b, BA1c, BA1d, BA1e samples ($15 \times 15 \times 15$ mm ± 2 mm dimension).

According to Table 2, all sets are subjected to cycles of T and rH in a fix CO_2 concentration atmosphere (see methods).

In addition, for each lithology, a capillary rising test with saline water (C_{GW}, C_{SW} and C_{TW}) was realized on a set. A capillary rising test with rainwater (C_{RW}) was realized on another set (Table 2).

Groundwater collected from Cagliari city aquifer was used for capillary rising test (C_{GW}) on marble, biomicrite and biolitite. Groundwater reproduces the infiltrations of a very shallow aquifer [61] that often floods the crypt of San Saturnino Basilica. Groundwater presents a total dissolved solids TDS = 491 mg/l.

Seawater was used for capillary rising test (C_{SW}) on basalts, Tyrrhenian sandstones and rhyodacites. Seawater reproduces the effects of sea spray on buildings of *Tharros* archaeological area and *Nora* Theatre placed few meter from shore. Seawater presents TDS = 37330 mg/l.

Thermal water collected at *Forum Traiani* baths was used for capillary rising test (C_{TW}) on rhyolites and reproduces the wettings of thermal NaCl-bearing hot water (54 °C) coming from natural springs still present inside the archaeological area [62,63]. Thermal water presents TDS = 826 mg/l.

Furthermore, rainwater capillary rising test with rainwater (C_{RW}, TDS = 42 mg/l), reproduces the rain.

Table 2
Set samples for FITOCLIMA ageing test. Every lithology has two set (1 and 2). A set consists of one 50x50x50mm ± 5 mm sample and five 15x15x15mm ± 2 mm samples (indicated in brackets).

Lithology	Set number	Set samples	Reproduced conditions
Sandstone	1	AT1 + (AT1a, AT1b, AT1c, AT1d, AT1e)	T, rH, CO_2, C_{RW}
	2	AT2 + (AT2a, AT2b, AT2c, AT2d, AT2e)	T, rH, CO_2, C_{SW}
Biomicrite	1	PC1 + (PC1a, PC1b, PC1c, PC1d, PC1e)	T, rH, CO_2, C_{RW}
	2	PC2 + (PC2a, PC2b, PC2c, PC2d, PC2e)	T, rH, CO_2, C_{GW}
Biolitite	1	PF1 + (PF1a, PF1b, PF1c, PF1d, PF1e)	T, rH, CO_2, C_{GW}
	2	PF2 + (PF2a, PF2b, PF2c, PF2d, PF2e)	T, rH, CO_2, C_{RW}
Marble	1	MA1 + (MA1a, MA1b, MA1c, MA1d, MA1e)	T, rH, CO_2, C_{GW}
	2	MA2 + (MA2a, MA2b, MA2c, MA2d, MA2e)	T, rH, CO_2, C_{RW}
Basalt	1	BA1 + (BA1a, BA1b, BA1c, BA1d, BA1e)	T, rH, CO_2, C_{SW}
	2	BA2 + (BA2a, BA2b, BA2c, BA2d, BA2e)	T, rH, CO_2, C_{RW}
Rhyodacite	1	AN1 + (AN1a, AN1b, AN1c, AN1d, AN1e)	T, rH, CO_2, C_{SW}
	2	AN2 + (AN2a, AN2b, AN2c, AN2d, AN2e)	T, rH, CO_2, C_{RW}
Rhyolite green *facies*	1	IGv1 + (IGv1a, IGv1b, IGv1c, IGv1d, IGv1e)	T, rH, CO_2, C_{TW}
	2	IGv2 + (IGv2a, IGv2b, IGv2c, IGv2d, IGv2e)	T, rH, CO_2, C_{RW}
Rhyolite red *facies*	1	IGr1 + (IGr1a, IGr1b, IGr1c, IGr1d, IGr1e)	T, rH, CO_2, C_{TW}
	2	IGr2 + (IGr2a, IGr2b, IGr2c, IGr2d, IGr2e)	T, rH, CO_2, C_{RW}

T = temperature, rH = relative humidity, CO_2 = carbon dioxide air concentration, C_{RW} = capillary rising with rainwater, C_{SW} = capillary rising with seawater, C_{GW} = capillary rising with groundwater, C_{TW} = capillary rising with thermal spring water.

In order to monitor the decay during the accelerated test in FITOCLIMA chamber, a series of physical–mechanical parameters (real density, imbibition coefficient, water open porosity, point load, tensile and compressive strength, sample section perimeters) were measured before (0 moment) and after the test (1 moment) verifying their relative variation (Δ%). The mass of the specimens was instead monitored at 15 days intervals including the particle-size distribution of decohesion residue by image analysis (iPSD). 3D micro-photogrammetry models of the samples (online available) allowed monitoring the external geometry and morphology before and after the test.

Inside SOLARBOX chamber eight samples with irregular dimensions (one for every lithology) subjected to only solar radiation were placed. The colour variations of those specimens were monitored at 15 days intervals allow to verify the trend of the chromatic alteration during the tests.

2.2. Methods

To control temperature, relative humidity and CO_2 air concentration a climatic chamber ARALAB FITOCLIMA S600PLH was used. The setting of the chamber took place by FITOLOG 600 control software.

Seasonal/daily variations of temperature (T) and humidity (rH) were obtained from Italian Air Force and Italian Civil Aviation Authority databases [64].

According to Table 3, Capo Frasca station (Central-Western Sardinia, 39°44′52.32″N, 8°27′24.99″E) and Cagliari-Elmas station (Southern Sardinia, 39°14′36.14″N, 9°03′36.78″E) are located only few Km from *Tharros/Forum Traiani* the first and San Saturnino Basilica/*Nora* Theatre the second. As for Table 3, the meteorological parameters T and rH of the two stations differ slightly as they are located at similar latitudes and altitude.

In order to obtain values of T and rH for FITOCLIMA setting, an arithmetic average of Capo Frasca and Cagliari-Elmas database was calculated (Table 3). The trends about daily and seasonal variations of T and rH are shown in Fig. 2.

For accelerating the test, a daily variation of T and rH is reproduced in 40 min of test (Fig. 2) and consequently a season is reproduced in 3600 min. In 6 months of test duration, samples underwent to 1.5 months of winter (Fig. 2a), 1.5 springtime (Fig. 2b), 1.5 summer (Fig. 2c) and 1.5 autumn (Fig. 2d). The 40 min cycle duration was carried out with the purpose of allowing the samples to equilibrate with surrounding environment.

During the test, a fix CO_2 air concentration of 403 ppm was set according to last available satellite observation on Sardinia (November 2016-January 2017, [65]).

In FITOCLIMA chamber, capillary rising test were conducted placing the samples in a plastic knurled support so that they set down on prominence ridges. In this way the water is able to rise through the sample.

Capillary rising is conducted applying 12 ml of water to 50 × 50 × 50 mm ± 5 mm sample and proportionally 1.6 ml to 15 × 15 × 15 mm ± 2 mm samples, once every 24 h of test. Those amounts of water are completely absorbed by the majority of the samples within 4/5 h.

For solar radiation a SOLARBOX3000 CO.FO.MEGRA chamber with 295–800 nm UV outdoor filter was used. Samples underwent 6 months of test with fix value of solar radiation of 700 W/m^2.

The 3D specimen models were performed on 50x50x50mm ± 5 mm samples by using Agisoft Photoscan 1.4.4. Software. For the reconstruction, a Nikon D3300 camera (24Mpx resolution) with 18–50 mm f/3.5–5.6 DC D was used. A total of 90 photos per sample were taken by building the upper and the lower half (chunks) of the model, subsequently combined using 4/5 paper targets applied on the specimen.

Petrographic determinations (OM) were carried out by optical polarised microscope Leitz Wetzlar on 30 μm thin sections realized according to UNI EN 12407:2019 [66]. Modal percentages on thin section were determined by synoptic table.

The mass values of the specimen during the ageing tests were obtained by Sartorius CP622 balance (instrumental tolerance of 0.01 g).

Setting of FITOCLIMA chamber was done by inserting into the control software FITOLOG 600 the arithmetic average data of the two meteorological stations (in italics)

In 40 min of test time (see X axis) has been reproduced the variation of T and rH during the day hours (see secondary X axis) of a typical Sardinia Csa climate winter day (a), springtime day (b), summer day (c) and autumn day (d).

Max/min values are also present in Table 3 and represent the arithmetic average of data from Capo Frasca and Cagliari-Elmas meteorological stations. Test was conducted with a fix 403 ppm CO_2 air concentration.

Was not possible to reach the min. winter temperature of 7 °C because the climatic chamber reaches a min. temp of 10 °C.

Particle-size distributions by image analysis (iPSD) were conducted according to the methods of Sitzia 2019 [59].

A 1200dpi scanning of the spread decohesion residue (Fig. 3a) was binarized and characterised (Fig. 3b) by ImageJ1.51 s Software. Each particle of residue, identified by its Feret diameter (ϕ_F) was classified as gravel (ϕ_F > 2 mm), sand (1/16 < ϕ_F < 2 mm), silt/clay (1/256 < ϕ_F < 1/16 mm) according to Wentworth [67].

Real density, imbibition coefficient and water open porosity were performed on 15 × 15 × 15mm ± 2 mm specimens according to the methods used to some authors [68] by using a Sartorius CPA324S balance and Quantachrome ULTRAPY1200e Pycnometer. Real density and water open porosity measurements have been done according to UNI EN 1936:2007 standard [69]. Imbibition coefficients were measured according to standard UNI EN 14617-1:2013 [70].

Point load index (Is_{50}) was determined by point load tester (Controls instrument D550) according to ISRM 1985 normative [71]. The compressive strength (R_C) and the tensile strength (R_T) were indirectly calculated from point load strength index according to Palmström [72].

Table 3
Max/Min temperature and relative humidity recorder in Capo Frasca and Cagliari-Elmas stations (period 1971–2000).

Capo Frasca meteorological station 39° 44′ 23.59″N, 8° 27′ 34.15″E	Season			
	Winter	Springtime	Summer	Autumn
Max average temp. (°C)	14.8	19.3	29.5	22.9
Min average temp. (°C)	6	9.5	18.2	13.4
Max average relative hum. (%)	94	88	84	88
Min average relative hum. (%)	74	74	72	74
Cagliari-Elmas meteorologyical station 39° 14′ 36.14″N, 9° 03′ 36.78″E	Season			
	Winter	Springtime	Summer	Autumn
Max average temp. (°C)	13.6	17.4	27	21.7
Min average temp. (°C)	8	10.9	19.5	15.1
Max average relative hum. (%)	88	79	72	78
Min average relative hum. (%)	68	65	60	72
Average data ((Capo Frasca + Cagliari-Elmas)/2)	Season			
	Winter	Springtime	Summer	Autumn
Max average temp. (°C)	14.2	18.4	28.3	22.3
Min average temp. (°C)	7.0	10.2	18.9	14.3
Max average relative hum. (%)	91	84	78	83
Min average relative hum. (%)	71	70	66	73

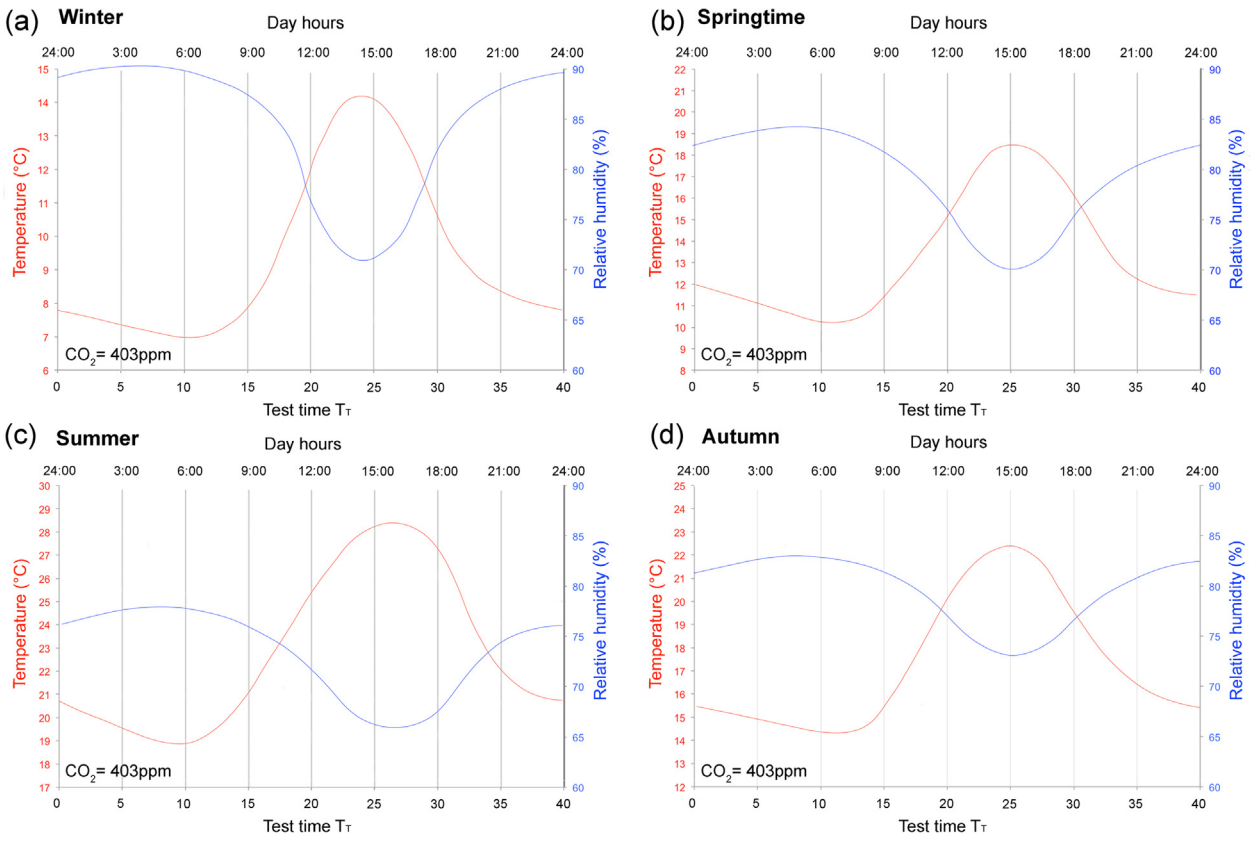

Fig. 2. Daily and seasonal trend of T and rH used for FITOCLIMA ageing.

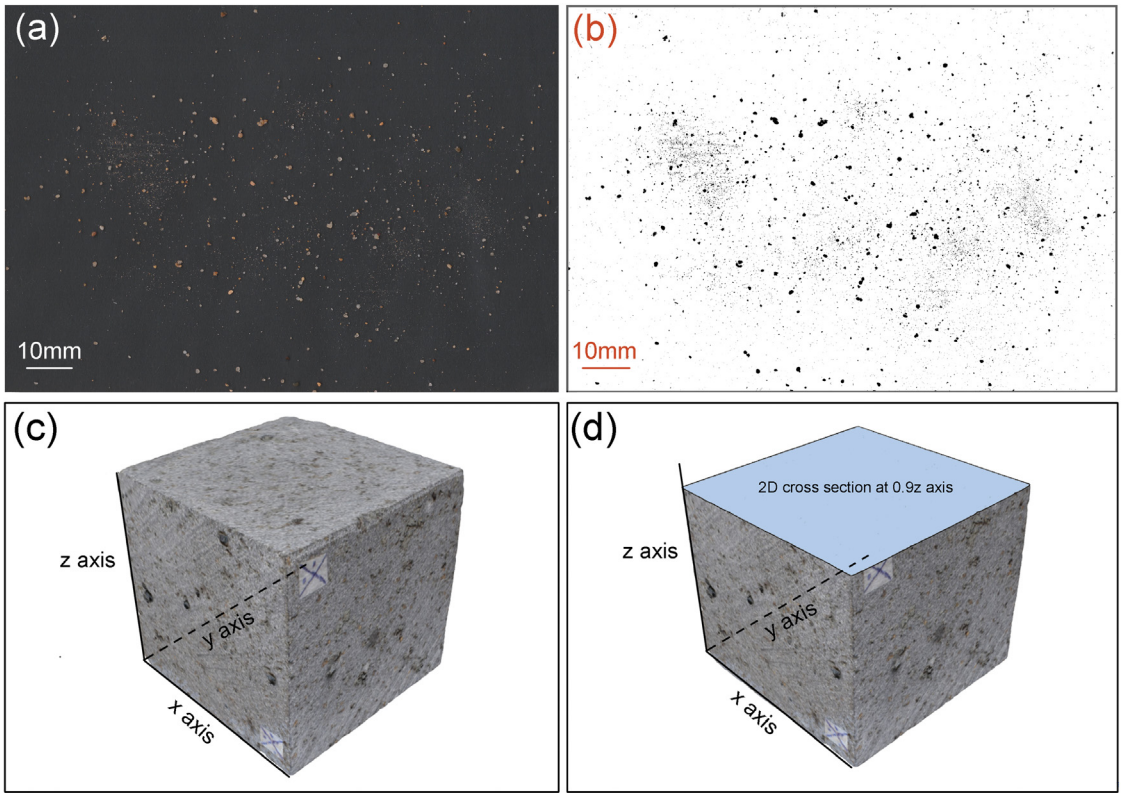

Fig. 3. Methodologies: (a) 1200 dpi scanning of the spread decohesion residue, (b) binarization of previous (a) image by ImageJ1.51 s Software, (c) example of BA1 sample before ageing test, (d) BA1 perimeter relative to xy 2D cross section at 0.9z axis.

Regarding morphological characterization, perimeters of the sample xy sections at 0.1z, 0,5z and 0.9z axis, where obtained from 3D models by Agisoft Photoscan 1.4.4. (see example in Fig. 3c, d).

Total dissolved solids of the waters have been measured with the help of a portable PANCELLENT TDS meter.

For colour monitoring of samples on SOLARBOX chamber, a portable DATACOLOR check II plus colorimeter, set with CIELAB (or CIE L*a*b*) colour system, has been used. Colour distance (ΔE_{ab}) was calculated according to CIE76 formula [73]: $\Delta E_{ab} = ((L_{Post} - L_{Pre})^2 + (a_{Post} - a_{Pre})^2 + (b_{Post} - b_{Pre})^2)^{0.5}$.

The relative variation (Δ %) of a generic property (P) before and after the test is calculated as:

$$\Delta\% = ((P_{Post} - P_{Pre})/P_{Pre})100.$$

3. Ageing test design: Test time (T_T), hypothetical outdoor exposure (T_A) and natural outdoor exposure (T_{AN})

The test time (T_T) is the period in which the samples are placed in climatic chamber. In our case, the experiments were conducted with T_T = 6 months in both chambers.

The hypothetical outdoor exposure (T_A) is the time defined by the product of test time and a hypothetical acceleration factor (see chapters 3.1 and 3.2). The term "hypothetical" means that the reproduction of the outdoor exposure on a climatic chamber is uncertain. A common criticism about ageing, in fact, indicates that the stone decay in the short term is clearly different from the natural decay in the long term. This is because dynamicity of processes is mainly due to the speed and stability of T and rH cycles that produce, for example, different evaporation rate, heat absorption than natural outdoor. Other differences are due to daily and seasonal averages of T and rH in climatic chamber, while in natural outdoor these parameters present variable trends and occasional extreme events.

Natural outdoor exposure time (T_{AN}) is the exposure time in real weathering environment that the samples need to reach the decay level reproduced on climatic chamber.

As it is possible to see after, the terms T_A and T_{AN} are always referred to specific monitored proprieties.

3.1. Hypothetical outdoor exposure for FITOCLIMA chamber test

During FITOCLIMA ageing, 2 climate parameters (e.g. T, rH) were cyclically reproduced in a CO_2-bearing atmosphere with the addition of capillary rising test. As above-mentioned in 40 min of test (T_T = 40 min) a daily cycle of T and rH was reproduced. Proportionally, during 6 months (T_T = 2.592 10^5 min) 6480 daily cycles corresponding to 6480/365 days $\approx$ 18 years of hypothetical outdoor exposure (T_A) were reproduced. In FITOCLIMA chamber, the relation between T_T and T_A is therefore T_A = F T_T. Where F is the hypothetical acceleration factor given by the ratio 18 years/0.5ye ars = 36.

3.2. Hypothetical outdoor exposure for SOLARBOX chamber test

During SOLARBOX aging, the solar irradiance was reproduced and defining a mathematic relation $T_T - T_A$.

Average global solar radiation of monuments location (Southern Sardinia) is 5.55 GJ/m^2/year corresponding to 15.20 MJ/m^2/day [74]. Only the 6% of this radiation falls in the ultraviolet region between 295 nm and 400 nm, or rather the wavelengths that create the most damage to materials surfaces. It means that southern Sardinia records a solar radiation of 0.91 MJ/m^2/day$_{295-400\ nm}$.

The average daily solar radiation of the international standard place (Miami, USA) is 1 MJ/m^2/day$_{295-400\ nm}$ [75].

Average daily radiation in Miami therefore is (1 MJ/m^2/day$_{295-400\ nm}$/0.91 MJ/m^2/day$_{295-400\ nm}$) = 1.1 times the average daily radiation in monument locations. For our experiment a radiation of 700 W/m^2 was selected.

According to SOLARBOX producer, chamber set at 700 W/m^2 with 295–800 nm UV outdoor filter, during one day of test (T_T = 1 day) reproduces 6.75 MJ/m^2 $_{295-400\ nm}$, corresponding to 6.75 days (T_A = 6.75 days) of hypothetical outdoor exposure in Miami and 6.75 days 1.10 = 7.4 days (T_A = 7.42 days) in monument locations. Therefore, the relation $T_T - T_A$ for monument location is the following:

T_A = F T_T (700 W/m^2 with 295–800 nm UV outdoor filter). Where F is the acceleration factor = 7.42.

It is important to underline that high temperature inside the SOLARBOX, as indicated by CO.FO.MEGRA, can accelerate the ageing speed. Considering a period of test duration T_T = 6 months, with a radiation of 700 W/m^2, the hypothetical solar outdoor exposure for monument location is $T_A \approx$ 3.7 years ($\approx$ 44.4 months).

4. Stone characterizations by optical mineralogy (OM)

According to Fig. 4a, sandstone presents microsparitic carbonate cement binding well-rounded clasts of quartz, feldspar, biotite, pyroxene and olivine. Rocks consist in a rich fossil fauna (e.g. coelenterates, algae, bivalves, gastropods). According to some authors [76] this sandstone has an age attributable to Tyrrhenian (0.126–0.0117 Ma).

The lithology was used for the construction of capitals, ashlars, columns and gutter beds at *Tharros* archaeological area.

Biomicrite (Fig. 4b) consists of a mud-supported limestone with 80% vol. of microcrystalline carbonate matrix, 5–15% vol. of clay (e.g. illite and kaolinite), 3% vol. of bioclasts and 2% vol. of allochems minerals (e.g. quartz, plagioclase, K-feldspar, biotite). According to some authors [77] this lithotype has a Miocenic age and was especially used in the realization of wall ashlars at San Saturnino Basilica.

Miocenic biolitite is characterised by 90% vol. of bioclasts, 8% vol. of microcrystalline carbonate cement (Fig. 4c) and 2% vol. of clay. The stone was used for the realization of wall ashlars, column basement and epistyles at San Saturnino Basilica.

Carrara marble (Fig. 4d) presents a mosaic texture of $CaCO_3$ crystals with sub-millimetric dimension. Secondary phases consist of quartz, muscovite, garnet, hematite, pyrite, magnetite, plagioclase and dolomite. The rock has a wide variety of uses such as colonnades, bases, capitals and wall ashlars at San Saturnino Basilica.

Basalts of Plio-Pleistocenic age (Fig. 4e) show porphyritic structure with mainly intersertal and subordinately pilotaxitic textures. The paragenesis consists of phenocrysts of plagioclase, olivine, ilmenite, magnetite and clinopyroxene.

The rock was used for architectural elements such as wall ashlars and floor paving at *Tharros* archaeological area.

Rhyodacites (Fig. 4f) of Oligo-Miocenic age, show a porphyritic structures and hyalopilitic texture. Paragenesis consists of phenocrysts of plagioclase, clinopyroxene, hornblende and magnetite. Rock is used for the construction of *Nora* Theatre's terraces and other secondary facilities in the archaeological area.

Rhyolites of Oligo-Miocenic age [78,79], (Fig. 4g, h) show different chromatic *facies* all characterised by porphyritic structure and eutaxitic texture. Phenocrysts are represented by plagioclase, feldspar, biotite and opaque. Groundmass is pumiceous-cineritic with frequent devitrification phases (e.g. celadonite, glauconite). Rhyolites are used in the construction of walls and paving at thermal baths of *Forum Traiani*.

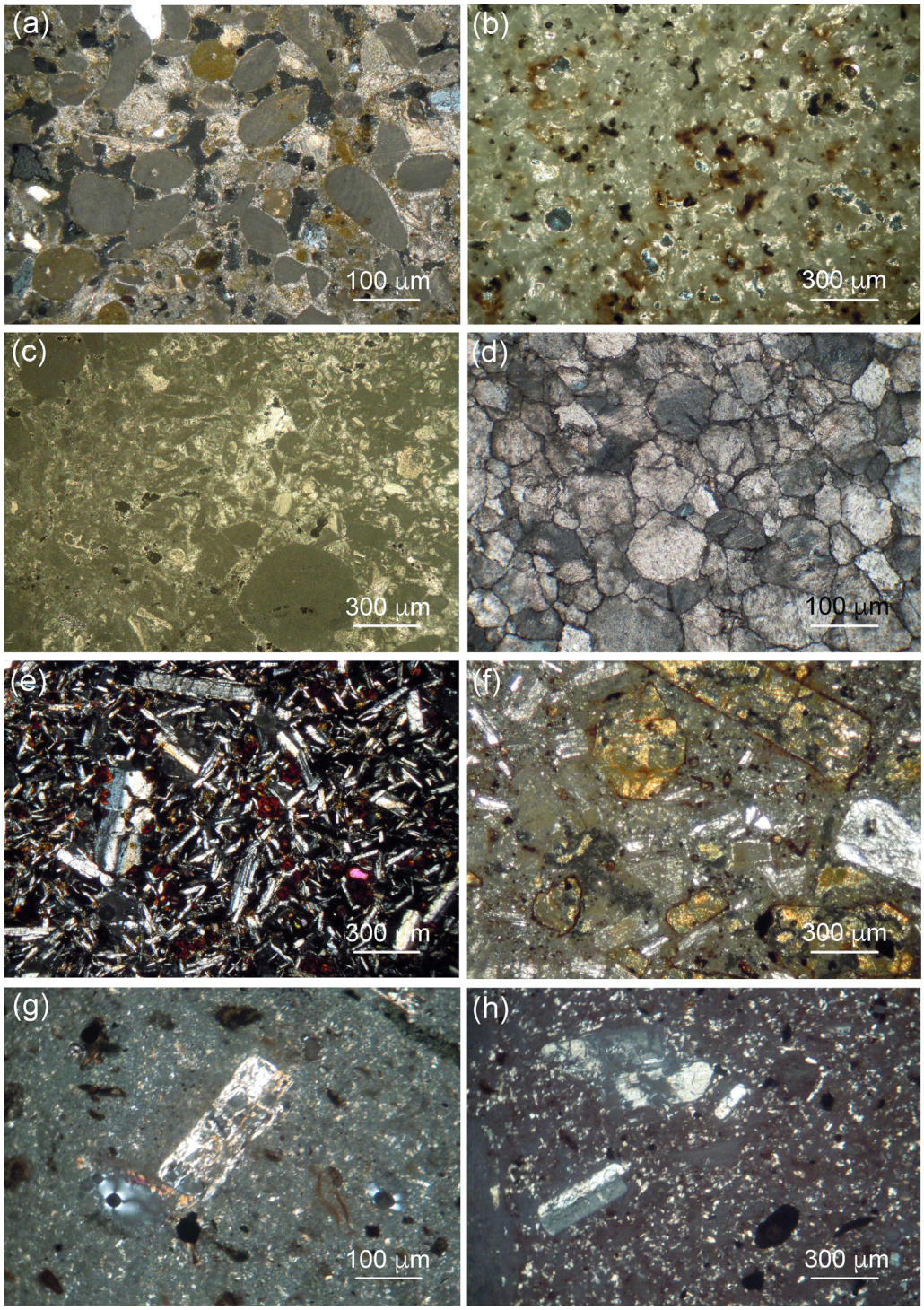

Fig. 4. Optical microscopy observation on stone building materials (a) sandstone, (b) biomicrite, (c) biolitite, (d) Carrara marble, (e) basalt, (f) rhyodacite, (g) green *facies* rhyolite, (h) red *facies* rhyolite. (For interpretation of the references to colour in this figure legend, the reader is referred to the web version of this article.)

5. Results and discussions

5.1. Sample mass monitoring and particle-size distribution of residue

Sample mass monitoring was performed on 50 × 50 × 50 mm ± 5 mm samples subjected to ageing test in FITOCLIMA chamber. Monitoring was conducted at T_T = 15 days interval. Results are show in Table 5 and Fig. 5.

In order to obtain a visual demonstration about the morphological modifications, in Table 4 are reported the links leading to 3D models before and after the ageing test.

The decay residue of the samples due to ageing is mainly represented by sands and secondly by silts/clay (Table 5).

By observing the graphs in Fig. 5, the mass loss is closely related to the salinity degree of the water used in the capillary rising. Other factors such as the type of salts dissolved in the solution

Table 4
Links to 3D digital models of 50x50x50mm ± 5 mm samples for FITOCLIMA chamber.

Sample	Lithology	Reproduced conditions	Link to 3D digital models	
			Pre test (T_T = 0 days)	Post test (T_T = 180 days)
AT1	Sandstone	T, rH, CO_2, C_{RW}	https://bit.ly/2EBZ4wn	https://bit.ly/38YukDR
AT2		T, rH, CO_2, C_{SW}	https://bit.ly/34HyTio	https://bit.ly/2PEtPHr
PC1	Biomicrite	T, rH, CO_2, C_{RW}	https://bit.ly/38Ys2EL	https://bit.ly/2PGuM1V
PC2		T, rH, CO_2, C_{GW}	https://bit.ly/2SbzeYc	https://bit.ly/35LGaiI
PF1	Biolitite	T, rH, CO_2, C_{GW}	https://bit.ly/35JvrVX	https://bit.ly/36W8qiR
PF2		T, rH, CO_2, C_{RW}	https://bit.ly/2Mc0JwP	https://bit.ly/2SagyYL
MA1	Marble	T, rH, CO_2, C_{GW}	N/A	N/A
MA2		T, rH, CO_2, C_{RW}	N/A	N/A
BA1	Basalt	T, rH, CO_2, C_{SW}	https://bit.ly/38ZYS8r	https://bit.ly/2Q4SmV7
BA2		T, rH, CO_2, C_{RW}	https://bit.ly/38UmHOZ	https://bit.ly/390C0W3
AN1	Rhyodacite	T, rH, CO_2, C_{SW}	https://bit.ly/2s5WAnt	https://bit.ly/2rXvIGn
AN2		T, rH, CO_2, C_{RW}	https://bit.ly/38Rfn6u	https://bit.ly/2ZbpAGl
IGv1	Rhyolite green *facies*	T, rH, CO_2, C_{TW}	https://bit.ly/2Z7Hw4O	https://bit.ly/35G3PB2
IGv2		T, rH, CO_2, C_{RW}	https://bit.ly/2Mc1juv	https://bit.ly/2reopcX
IGr1	Rhyolite red *facies*	T, rH, CO_2, C_{TW}	https://bit.ly/36Q9BA8	https://bit.ly/2EE263j
IGr2		T, rH, CO_2, C_{RW}	https://bit.ly/2SclJYh	https://bit.ly/2EzQONF

N/A = not available, photogrammetry cannot be done on crystalline rocks. The reason is that the strong light reflection of the individual crystals does not allow the software to establish fixed reference points.
T = temperature, rH = relative humidity, CO_2 = carbon dioxide air concentration, C_{RW} = capillary rising with rainwater, C_{SW} = capillary rising with seawater, C_{GW} = capillary rising with groundwater, C_{TW} = capillary rising with thermal spring water.

Table 5
Loss mass of 50x50x50mm ± 5 mm samples for FITOCLIMA chamber and image particle-size (iPSD) of decay residue. G = gravel, S = sand, S/C = silt/clay. T = temperature, rH = relative humidity, CO_2 = carbon dioxide air concentration, C_{RW} = capillary rising with rainwater, C_{SW} = capillary rising with seawater, C_{GW} = capillary rising with groundwater, C_{TW} = capillary rising with thermal spring water.

Sample	Lithology	Reproduced conditions	Mass (%)		*Total loss mass M_T (%)*	*Average daily loss mass M_D (%)*	iPSD decay residue (%)		
			Pre test (T_T = 0 days)	Post test (T_T = 180 days)			G	S	S/C
AT1	Sandstone	T, rH, CO_2, C_{RW}	100	99.26	*0.74*	*0.004*	0.4	74.9	24.7
AT2		T, rH, CO_2, C_{SW}	100	95.21	*4.79*	*0.026*			
PC1	Biomicrite	T, rH, CO_2, C_{RW}	100	97.62	*2.38*	*0.013*	0	76.4	23.6
PC2		T, rH, CO_2, C_{GW}	100	96.12	*3.88*	*0.021*			
PF1	Biolitite	T, rH, CO_2, C_{GW}	100	98.96	*1.04*	*0.006*	0	73.5	26.5
PF2		T, rH, CO_2, C_{RW}	100	99.70	*0.30*	*0.002*			
MA1	Marble	T, rH, CO_2, C_{GW}	100	99.67	*0.33*	*0.002*	0	70	30
MA2		T, rH, CO_2, C_{RW}	100	99.75	*0.25*	*0.001*			
BA1	Basalt	T, rH, CO_2, C_{SW}	100	99.39	*0.61*	*0.003*	0	65	34
BA2		T, rH, CO_2, C_{RW}	100	99.71	*0.29*	*0.002*			
AN1	Rhyodacite	T, rH, CO_2, C_{SW}	100	99.63	*0.37*	*0.002*	0	56.8	43.2
AN2		T, rH, CO_2, C_{RW}	100	99.81	*0.19*	*0.001*			
IGv1	Rhyolite green *facies*	T, rH, CO_2, C_{TW}	100	99.81	*0.19*	*0.001*	0	56.1	43.9
IGv2		T, rH, CO_2, C_{RW}	100	98.97	*1.03*	*0.006*			
IGr1	Rhyolite red *facies*	T, rH, CO_2, C_{TW}	100	99.79	*0.21*	*0.001*	0	64.9	35.1
IGr2		T, rH, CO_2, C_{RW}	100	99.83	*0.17*	*0.001*			

and their crystallization pressure influence the decay by crystallization-solubilisation which induces the decohesion of the stone and the consequent loss of mass. In particular, sulphates present in thermal and seawater are mainly responsible for the stone decay [80,81]. Physical-mechanical features of the rocks (e.g. open porosity, diameter of the pores, permeability, particle-size, cohesion degree), also influence the decay and the consequent disaggregation.

In this work, all samples subjected to ageing show a loss of mass, but an increase due to saline deposition inside the pores framework could be recorder in the first steps of ageing [82]. In our case-study the decohesion process is always predominant.

In Fig. 5a AT2 sandstone sample is affect by capillary rise with seawater whereas AT1 is affect by the capillary rise with rainwater. In Table 5 is recorded a total loss mass percentage Δ_{MT} = 0.74% and 4.79% for AT1 and AT2 respectively. The average daily test loss mass is 0.004% in AT1 and 0.026% for AT2 (Table 5).

In this lithology mass loss occurs due to granular decohesion with a residue consisting of 0.4% gravel, 74.9% sand and 24.7% silt/clay (Table 5).

The Fig. 5b shows the loss mass trend of PF1 and PF2 biolitites. As you can notice, the greatest mass loss is attributed to the sample PF1 (Δ_{MT} = 1.04%) while in PF2 Δ_{MT} = 0.3% (Table 5). As visible in Fig. 5b a large mass loss on PF1 occurs at T_T = 135 days when a large fragment of sample detached (exfoliation) from a pre-existing fracture. The detachment furrow is well visible in the 3D post-test reconstruction (links in Table 4).

In biomicrites, the trends of PC1 and PC2 loss masses (Fig. 5b) are represented by curves with variable inclination due to at least three decay typologies also observed at San Saturnino Basilica [59]

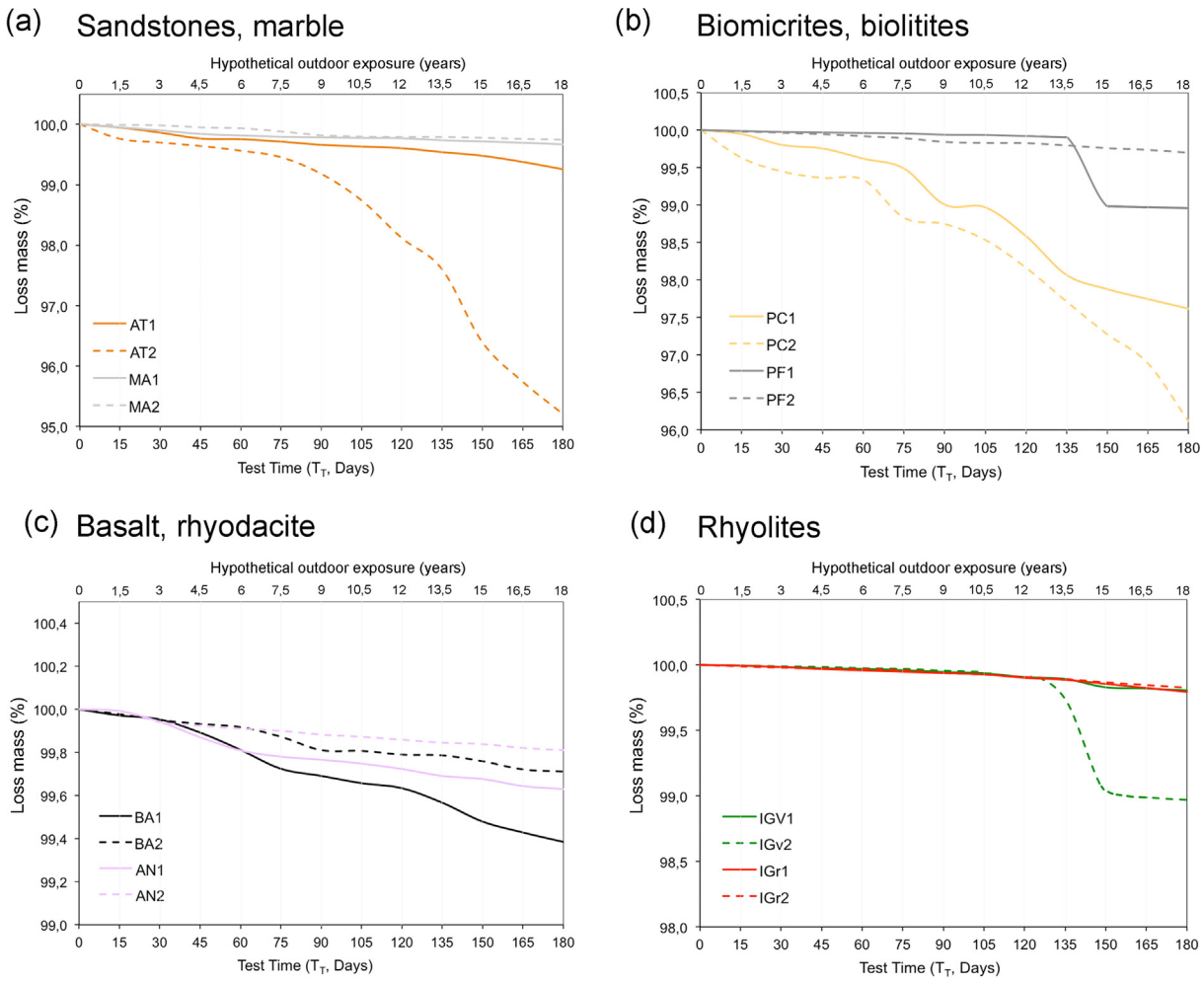

Fig. 5. Loss mass trends of 50 × 50 × 50 mm ± 5 mm samples for FITOCLIMA chamber.

(e.g. granular decohesion, exfoliation, differential erosion) that heavily modify the morphology of the specimens (see link to 3D reconstruction on Table 4).

In PC2 sample, subjected to saline groundwater capillary rising, the daily test relative mass loss Δ_{MD} = 0.021% with a total weight loss Δ_{MT} = 3.88% (Table 5). In PC1 subjected to rainwater capillary rising Δ_{MD} = 0.013% and Δ_{MT} = 2.38% were obtained. Also in this case, saline groundwater on PC2 determines a greater mass loss respect than PC1.

Decohesion of biomicrites at San Saturnino Basilica is today very clear and problematic. Experiments carried out inside the church, showed a ground residue deposition of average 470 g/m^2/year in the area of the apse [59].

It has also been highlighted by hydrogeological prospections as the Cagliari city aquifer is subjected to seawater intrusions.

For this reason, the groundwater used in capillary rising tests contains NaCl. As demonstrated by some authors, this salt has a high crystallization pressure in supersaturated solutions at 25 °C [81,83]. However, it seems to create less damage than sulphates and carbonates because it is easier to wash out.

On the others lithologies such as marbles (Fig. 5a), rhyolites (Fig. 5c), basalts and rhyodacites (Fig. 5d), the differences of mass loss between samples subject to saline and meteoric water capillary rising is less evident due to higher mechanical strengths of the stones.

Carrara marble is very resistant to ageing test showing only Δ_{MT} = 0.33% and 0.25% for MA1 and MA2 respectively (Table 5). Rock decay consists of a weak decohesion with residue composed by 70% sand and 30% silt/clay.

Green *facies* rhyolites show an opposite trend of mass loss, where Δ_{MT} = 0.19% in IGv1 subjected to thermal water capillary rising and Δ_{MT} = 1.03% in IGv2 subjected to rainwater capillary rising. This is due to a loss of two fragments (exfoliation) on IGv2 at 120 < T_T < 150 days in the upper part of the sample, also visible into 3D model (Table 4). Exfoliation processes has been also identified on *Forum Traiani* structures associated with decohesion. This last decay only affects the pumiceous-cineritic fraction of the rhyolites causing a differential erosion between groundmass and fragments of glass, pumice and crystal.

5.2. Morphologic monitoring: Perimeters of xy cross sections at 0.1, 0.5, 0.9 z axis

The monitoring of xy cross section perimeters at 0.1, 0.5 and 0.9z axis, was conducted on 50x50x50mm ± 5 mm samples for FITOCLIMA chamber. Z axis identifies the vertical side of the specimen according to the orientation of 3D models, the same that the sample had in the climatic chamber (example in Fig. 3c, d).

Monitoring was performed at pre and post test steps. As show in Table 6, a decrease of perimeters and, consequently, resistant sections only occurred in the samples of sandstone, biomicrite and biolitite.

About remaining lithologies, characterised by higher mechanical strength and cohesion, the perimeters remain unchanged or

Table 6
Xy section perimeters at 0.1, 0.5 and 0.9z of 50 × 50 × 50 mm ± 5 mm samples for FITOCLIMA chamber.

Sample	Lithology	Reproduced conditions	Perimeters (mm)						$\Delta p_{0.1z}$ (%)	$\Delta p_{0.5z}$ (%)	$\Delta p_{0.9z}$ (%)
			Pre test (T_T = 0 days)			Post test (T_T = 180 days)					
			p 0.1z	p 0.5z	p 0.9z	p 0.1z	p 0.5z	p 0.9z			
AT1	Sandstone	T, rH, CO_2, C_{RW}	203.4	207.5	217.8	201.2	206.8	217.1	*−1.08*	*−0.34*	*−0.32*
AT2		T, rH, CO_2, C_{SW}	205.8	217	206.5	198.5	212.6	204.3	*−3.55*	*−2.03*	*−1.07*
PC1	Biomicrite	T, rH, CO_2, C_{RW}	201.2	199.3	198.4	197.8	198.8	195.3	*−1.69*	*−0.25*	*−1.56*
PC2		T, rH, CO_2, C_{GW}	204.7	201.5	207.5	202.8	198.8	203.9	*−0.93*	*−1.34*	*−1.73*
PF1	Biolitite	T, rH, CO_2, C_{GW}	209.1	210.4	208.1	199.6	210.4	208.1	*−4.54*	*0*	*0*
PF2		T, rH, CO_2, C_{RW}	211.1	211.1	209.8	211.1	211.1	209.8	*0*	*0*	*0*
MA1	Marble	T, rH, CO_2, C_{GW}	N/A	N/A	N/A	N/A	N/A	N/A	*N/A*	*N/A*	*N/A*
MA2		T, rH, CO_2, C_{RW}	N/A	N/A	N/A	N/A	N/A	N/A	*N/A*	*N/A*	*N/A*
BA1	Basalt	T, rH, CO_2, C_{SW}	203.7	201.4	206.1	203.7	201.4	206.1	*0*	*0*	*0*
BA2		T, rH, CO_2, C_{RW}	200.6	198.2	198.4	200.6	198.2	198.4	*0*	*0*	*0*
AN1	Rhyodacite	T, rH, CO_2, C_{SW}	205.2	204.2	203.1	205.2	204.2	203.1	*0*	*0*	*0*
AN2		T, rH, CO_2, C_{RW}	199.5	199.5	200.8	198.8	199.5	200.8	*0*	*0*	*0*
IGv1	Rhyolite green *facies*	T, rH, CO_2, C_{TW}	201	199.5	195.3	201	199.5	195.3	*0*	*0*	*0*
IGv2		T, rH, CO_2, C_{RW}	198	204.5	194.4	194.4	200.6	194.4	*0*	*0*	*0*
IGr1	Rhyolite red *facies*	T, rH, CO_2, C_{TW}	188.6	193.1	195.1	188.6	193.1	195.1	*0*	*0*	*0*
IGr2		T, rH, CO_2, C_{RW}	191.2	191	191.5	191.2	191	191.5	*0*	*0*	*0*

N/A = not available, photogrammetry cannot be done on crystalline rocks.
T = temperature, rH = relative humidity, CO_2 = carbon dioxide air concentration, C_{RW} = capillary rising with rainwater, C_{SW} = capillary rising with seawater, C_{GW} = capillary rising with groundwater, C_{TW} = capillary rising with thermal spring water.

the variations are so small such that they cannot be identified by photogrammetry.

In sandstones AT1 and AT2, a progressive loss mass for decohesion also visible in Fig. 5a, causes the perimeter reduction especially at the base of the samples (0.1z) more affected by capillary rise.

At 0.5 and 0.9z perimeter reduction in both samples is lower. It is also observed that the decrease of perimeters at 0.1, 0.5 and 0.9z is more relevant in AT2 sample subject to capillary rise with seawater.

In PC1 and PC2 biomicrite, the decay process (Fig. 5b) causes a progressive curvature of the sharp edges of the sample, in fact, perimeters decrease at 0.1 and 0.9z. In PC2 sample subject to capillary rise with groundwater, it is also observed that the decrease of perimeters at 0.5 and 0.9z ($\Delta p_{0.5z}$ = −1.34% and $\Delta p_{0.9z}$ = −1.73%) is more relevant than PC1 ($\Delta p_{0.5z}$ = −0.25% and $\Delta p_{0.9z}$ = -1.56%, Table 6). On PF1 biolitite an exfoliation process at the lay face of the sample caused a strong perimeter reduction ($\Delta p_{0.1z}$ = −4.54%, Table 6).

The process of base perimeter and section reduction is *in situ* extremely diffuse on sandstones colonnade at *Tharros* archaeological area, on walls at San Saturnino Basilica and *Forum Traiani*. In some case has been detected, a reduction of the structural element base section up to 25% respect than the original one. This erosion process induces reduction of the resistant surface and a worsening of the static loads diffusion of the building, with consequent problems of loads eccentricity [84].

On monuments, the only capillary rising could be not the only cause of base section erosion but, in the lower part of the wall, it is often accentuated by the rebound water coming from the roof that hits the soil.

Although no perimeter variations have been identified on rhyolite samples in this work, at *Forum Traiani* the stone ashlars are subject to strong morphological deformations of mainly coving (single alveolus) [85] and rarely contour scaling [86].

5.3. Monitoring of physical-mechanical characteristics

The physical-mechanical properties were measured on the 5 15 × 15 × 15mm ± 2 mm specimens before and after FITOCLIMA ageing test. Results are show in Tables 7 and 8.

The physical-mechanical properties were measured on only sets affected to saline water capillary rising (e.g. C_{SW}, C_{GW}, C_{TW}, Table 2). The values in Tables 7 and 8, therefore, represent an arithmetic average of 5 measurements.

In physical properties, both decrease and increase are observed in response to the physical-chemical changes occurred during ageing.

A real density ρ_R increase was observed on biolitite, basalt and rhyolites (Table 7) probably be due to a mineral deposition inside the inner pores together with a parallel decrease of water open porosity.

Some authors [14] have observed that increase of real density on samples subjected to F-T ageing and salt crystallization (UNI EN 12370), is due to an overall decrease of porosity especially in the pore range < 0.1–1 μm.

In this work, a real density decrease is observed on sandstones, biomicrites, marbles and riodacites, also in this case correlated with porosity increase trend. Decreases and increases of ρ_R can be also related to various processes as sulphation (especially on limestone and sandstone) oxidations and formations of efflorescences [87].

Increases of the imbibition coefficient Δ Cl_w are observed on all lithology but biolitite (−26.47%) and rhyolites (−9.4 and −0.44%). The imbibition coefficient mainly increases due to a parallel increase of water open porosity.

This is due to the crystallization pressure that probably causes a general enlargement of open pores leading to the formation of micro cracks, together with a changing of pores tortuosity.

Salts crystallization/solubilisation on porous network, in fact, occurs according to daily and seasonal temperature and relative humidity cycles to which the samples are subjected during six months of ageing test. It was observed that in the early stages of the tests, especially on biomicrites, the decohesion residue adheres to the surface of the sample forming a ≈ 200 μm thickness "noble patina" as observed to some authors [88,89] protecting the stone from atmospheric agents and solution circulation. During the dry season in FITOCLIMA, this patina dries up and becomes compact. During the winter cycle, indeed, a general increase in relative humidity wets the patina leading to its decohesion.

Table 7
Data of real density, imbibition coefficient and water open porosity measured before and after FITOCLIMA ageing test.

Lithology	Reproduced conditions		Pre test (T_T = 0 days)			Post test (T_T = 180 days)			$\Delta\rho_R$ (%)	ΔCl_W (%)	$\Delta\phi H_2O$ (%)
			Real density ρ_R (g/cm^3)	Imbibition coefficient Cl_w (%)	Water open porosity ϕH_2O (%)	Real density ρ_R (g/cm^3)	Imbibition coefficient Cl_w (%)	Water open porosity ϕH_2O (%)			
Sandstone	T, rH, CO_2, C_{SW}	M. A.	2.67	19.95	32.76	2.66	20.75	33.13	*−0.29*	*3.99*	*1.12*
		D. S.	*0.01*	*2.12*	*2.29*	*0.02*	*1.31*	*1.12*			
Biomicrite	T, rH, CO_2, C_{GW}	M. A.	2.7	8.68	18.29	2.68	9.45	19.58	*−0.62*	*8.88*	*7.14*
		D. S.	*0.01*	*0.97*	*1.61*	*0.01*	*1.02*	*1.6*			
Biolitite	T, rH, CO_2, C_{GW}	M. A.	2.71	2.98	7.37	2.73	2.19	5.56	*0.79*	*−26.47*	*−24.54*
		D. S.	*0.01*	*0.25*	*0.6*	*0.01*	*0.33*	*0.8*			
Marble	T, rH, CO_2, C_{GW}	M. A.	2.72	1.15	2.99	2.71	1.26	3.27	*−0.31*	*9.8*	*9.22*
		D. S.	*0.01*	*0.18*	*0.45*	*0.01*	*0.48*	*1.18*			
Basalt	T, rH, CO_2, C_{SW}	M. A.	2.82	4.46	10.58	2.83	4.79	11.38	*0.14*	*7.46*	*7.59*
		D. S.	*0.01*	*1.17*	*2.44*	*0.01*	*0.95*	*2*			
Rhyodacite	T, rH, CO_2, C_{SW}	M. A.	2.67	11.1	22.02	2.66	14.09	26.97	*−0.38*	*27*	*22.48*
		D. S.	*0.01*	*0.47*	*0.85*	*0.02*	*1.39*	*2.16*			
Rhyolite green *facies*	T, rH, CO_2, C_{TW}	M. A.	2.56	18.94	30.58	2.57	17.16	28.51	*0.64*	*−9.4*	*−6.77*
		D. S.	*0.03*	*3.45*	*3.61*	*0.01*	*2.35*	*3.31*			
Rhyolite red *facies*	T, rH, CO_2, C_{TW}	M. A.	2.57	20.55	32.57	2.59	20.46	32.52	*0.74*	*−0.44*	*−0.17*
		D. S.	*0.04*	*3.11*	*3.36*	*0.03*	*3.09*	*2.83*			

Each value represents the arithmetic average of the 5 specimens 15x15x15mm ± 2 mm only belonging to the sample sets affected by capillary rising with saline waters (e.g. marine water, groundwater and thermal water). M.A. = arithmetic average, D.S. = standard deviation. T = temperature, rH = relative humidity, CO_2 = carbon dioxide air concentration, C_{SW} = capillary rising with seawater, C_{GW} = capillary rising with groundwater, C_{TW} = capillary rising with thermal spring water.

A decreasing of the water open porosity observed on biolitite (-24.54%) and green/red *facies* rhyolites (−6.77, −0.17 respectively) could derive from a pore obstruction due to salt deposition on porous network. Those salts mainly derive from capillary rising saline water and secondly from stone leaching.

Mechanical characterization of rocks available in Table 8, shows a general decrease of point load index and proportionally of the compression and tensile strengths. Decreases are included in a range $-1.57 < \Delta Is_{50} = \Delta R_C = \Delta R_T < -33.33\%$ on sandstone, biomicrite, marble, basalt and rhyodacite, probably related to an increase of water open porosity (Table 7).

In this work, as indicated in literature, ageing on stone causes, in the majority of the stones, a decrease of mechanical resistances [90]. Some authors indicate a model of prediction of uniaxial compressive strength for deteriorated rocks due to freeze–thaw [91]. In another work [92] seems that compression strength during F-T cycle, C-H and W-T (wet and dry) of ageing is subjected to increases. Also in our case the sample of biolitite show a mechanical strength enhance ($\Delta Is_{50} = \Delta R_C = \Delta R_T = 0.4\%$) at the finish of ageing test. It is probable that if the test had been continued beyond six months we will have registered a probable decrease mechanical parameters. Fluctuations of mechanical strengths could be due to continuous modifications of pores size, distributions and degree of interconnections that could have create a *porosity optimum* [93].

5.4. Colour monitoring

CIELAB colour space (or CIE L*a*b*) variations were measured on SOLARBOX samples at T_T = 15 days interval (Fig. 6). Data about pre/post lightness, a, b colours and colour distance ΔE_{ab} are shown in Table 9.

As in Fig. 6, some lithologies (e.g. biomicrite, biolitite, marble, basalt and green *facies* rhyolite) show a discrete variation of L, a, b parameters just at the early stages of the test ($0 < T_T < 30$ days). In all samples, the trend of L, a, b parameters (Fig. 6) is characterised by fluctuations.

The same fluctuation trend has been documented on the paintings by some authors [94] and it is due to a series of reaction that take place inside the SOLARBOX chamber. Solar exposition of the stone could also causes a gloss decrease [95].

In this works, increases of lightness are observed on sandstone, biomicrite, basalt and rhyodacite corresponding to variations towards whiter colours (Table 9). Lightness decreases are very evident on marble and rhyolites ($\Delta_L\%$ = −3.36, −3.36 and −4.15, Table 9) corresponding to darkening. This last process had been already identified on marble by some authors [96]. Marbles are, in fact, prone to discoloration, turning into creamier colours [97]. On other limestones, and in particular in travertines, authors [96] recorded a bleaching of the stone due to prolonged exposure to sunlight.

Table 8
Data of point load, compressive and tensile strength measured before and after FITOCLIMA ageing test. Each value represents the arithmetic average of the 5 specimens 15x15x15mm ± 2 mm only belonging to the sample sets affected by capillary rising with saline waters (e.g. marine water, groundwater and thermal water). M.A. = arithmetic average, D.S. = standard.

Lithology	Reproduced conditions		Pre test (T_T = 0 days)			Post test (T_T = 180 days)			$_{\Delta}Is_{50} = {}_{\Delta}R_C = {}_{\Delta}R_T$ (%)
			Point load strength I_{s50} (MPa)	Compression strength R_C (MPa)	Tensile strength R_T (MPa)	Point load strength I_{S50} (MPa)	Compression strength R_C (MPa)	Tensile strength R_T (MPa)	
Sandstone	T, rH, CO_2, C_{SW}	M. A.	0.69	9.68	0.86	0.46	6.46	0.58	−33.33
		D.S.	*0.12*	*1.71*	*0.15*	*0.09*	*1.22*	*0.11*	
Biomicrite	T, rH, CO_2, C_{GW}	M. A.	1.33	18.66	1.67	1.08	15.06	1.34	−18.79
		D.S.	*0.07*	*0.96*	*0.09*	*0.09*	*1.3*	*0.12*	
Biolitite	T, rH, CO_2, C_{GW}	M. A.	7.43	104.05	9.29	7.46	104.43	9.32	0.4
		D.S.	*0.94*	*13.21*	*1.18*	*0.99*	*13.91*	*1.24*	
Marble	T, rH, CO_2, C_{GW}	M. A.	3.18	44.52	3.97	3.13	43.78	3.91	−1.57
		D.S.	*0.35*	*4.93*	*0.44*	*0.29*	*4.05*	*0.36*	
Basalt	T, rH, CO_2, C_{SW}	M. A.	7.04	140.76	8.8	6.91	96.7	8.63	−1.84
		D.S.	*0.9*	*17.96*	*1.12*	*0.26*	*3.59*	*0.32*	
Rhyodacite	T, rH, CO_2, C_{SW}	M. A.	7.16	143.13	8.95	6.74	94.3	8.42	−5.86
		D.S.	*1.29*	*25.74*	*1.61*	*0.71*	*10*	*0.89*	
Rhyolite green *facies*	T, rH, CO_2, C_{TW}	M. A.	2.49	34.81	3.11	2.27	31.83	2.84	−8.83
		D.S.	*0.25*	*3.45*	*0.31*	*0.38*	*5.28*	*0.47*	
Rhyolite red *facies*	T, rH, CO_2, C_{TW}	M. A.	2.05	28.67	2.56	1.54	21.6	1.93	−24.87
		D.S.	*0.57*	*7.93*	*0.71*	*0.24*	*3.37*	*0.3*	

Deviation. T = temperature, rH = relative humidity, CO_2 = carbon dioxide air concentration, C_{SW} = capillary rising with seawater, C_{GW} = capillary rising with groundwater, C_{TW} = capillary rising with thermal spring water

Decreases of a colour, corresponding to variations towards red tonalities, are detected on sandstone, biomicrite, biolitite, rhyodacite and rhyolites. Increases of a colour are especially noted on marble (Δ_a% = 11.54%) and basalt (Δ_a% = 46.15%, Table 9, Fig. 6) corresponding to variations towards green tonalities.

It has been demonstrated how a colour tends to decrease on serpentinites exposed to solar light together with a decrease of Chroma and Hue [98].

The opposite b colour decreases in all ours lithologies (Fig. 6, Table 9), highlighting variations towards blue tonalities.

The solar radiation test demonstrates how the colour variation results in a small range $1.41 < \Delta E_{ab} < 1.47$ on sandstone, basalt, rhyodacite and $2.38 < \Delta E_{ab} < 3.53$ on biolitite, biomicrite, marble, rhyolites (Table 9).

According to the CIE76 ΔE_{ab} system, the human eyes can percept a colour distance over to a determinate value of JND (just-noticeable difference) over ≈2.37 [101]. Therefore, colour variation according to perceptual acuity of people [66] can only seen on biolitite, biomicrite, marble, and red *facies* rhyolite.

Some authors [99,100] indicate that the colour variations of the stone exposed to sunlight, in particular to UV rays, are due to the oxidation of organic matter, iron (from Fe^{+2} to Fe^{+3}), pyrite (FeS_2) and chromite ($FeCr_2O_4$) when present.

6. Conclusions

Ageing test on stones, has caused a slight loss mass together with a weakening of mechanical proprieties. The resistance of rock to ageing is strictly related to mechanical characteristics, especially in basalt, biolitite, marble and rhyodacite or to the welding degree of rhyolites. Other features inducing decay are given by the permeability and moisture retention.

On biomicrite and sandstones ageing causes the strongest decay mainly due to the rock fabric and texture. Even if these stones have low resistance, were widely used as building materials because of their workability and availability near the monuments.

Ageing together with capillary rising test show how the position of the stone on monuments is crucial in the decay especially when the stone is placed at the lower part of the walls. Here ashlars suffer of capillary rising from soil or from thermal source in the case of Forum Traiani. It has been demonstrated that rainwater, according to its low salt content, seems to be less damaging, but in this case experiments doesn't reproduce the mechanical action of rain drop on stones.

Today, at San Saturnino Basilica, and *Tharros* archaeological area as well as in other building of Mediterranean area, biolitite and sandstones need of consolidation interventions. For this reasons it is crucial to predict the stone decay by ageing test.

It is important to underline that ageing test design proposed in this research aims to detect some qualitative indications about decay/chromatic alteration to which the materials would be subject *in situ*.

Although a hypothetical outdoor exposure have been formulated, it is not possible to assume that Δ values of physical–mechanical, and morphologic properties after ≈18 years and ΔE_{ab} chromatic values after ≈3.7 years of natural outdoor exposure coincide with the ones reproduced in 6 months of test. As abovementioned, this happens because the accelerated and natural processes are not parallel.

As in our case, also trying to fully reproduce all the characteristics of a given climate, the biggest problem is the wide variability and complexity of natural outdoor exposures.

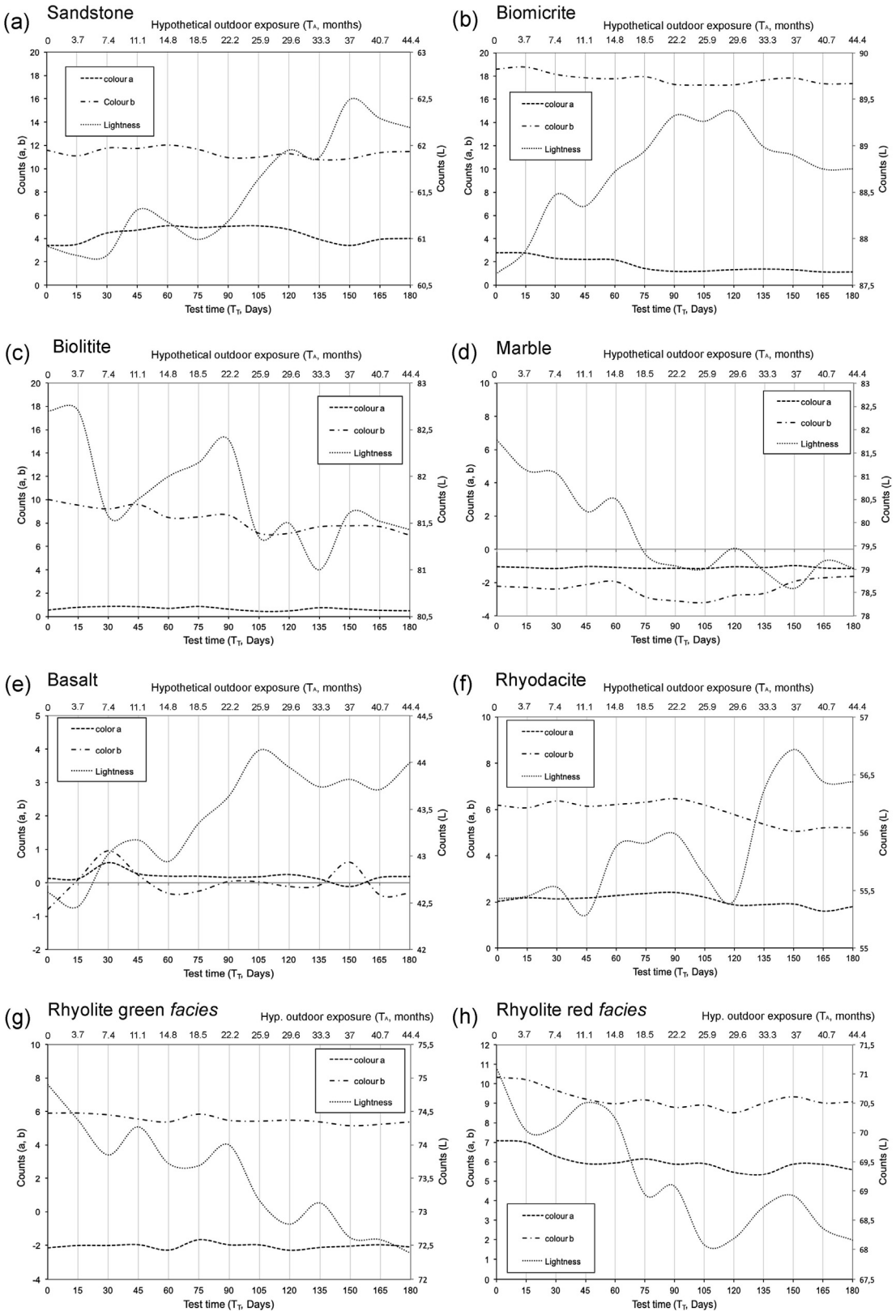

Fig. 6. Trend of CIELAB lightness, a and b colour during 6 months of ageing test in SOLARBOX chamber.

As above mentioned, although artificial cyclic exposures tend to be more severe than natural exposures it is necessary to highlight that for example, the experiment overlooks the damage of biodeterioration.

A possible way to verify, in terms of monitored properties:

- If Δ values obtained after 6 months of accelerate ageing correspond to Δ values obtained after ≈18 years or ≈3,7 years (test confidence)
- In how much time Δ values obtained after 6 months of accelerate ageing are reached in natural outdoor exposure

Table 9
Data of lightness, a/b colours and colour distance of SOLARBOX samples.

Lithology	Reproduced conditions	Pre test lightness L	Post test lightness L	ΔL (%)	Pre test a colour a	Post test a colour a	Δa (%)	Pre test b colour b	Post test b colour b	Δb (%)	Colour distance ΔE_{ab}
Sandstone	Solar radiation	60.92	62.19	*2.08*	3.39	4	*17.99*	11.59	11.48	*−0.95*	1.41
Biomicrite		87.62	88.75	*1.29*	2.79	1.11	*−60.22*	18.59	17.33	*−6.78*	2.38
Biolitite		82.7	81.43	*−1.54*	0.55	0.48	*−12.73*	10	6.96	*−30.4*	3.3
Marble		81.77	79.02	*−3.36*	−1.04	−1.16	*11.54*	−2.22	−1.62	*−27.03*	2.82
Basalt		42.61	44	*3.26*	0.13	0.19	*46.15*	−0.79	−0.31	*−60.76*	1.47
Rhyodacite		55.43	56.44	*1.82*	2.03	1.81	*−10.84*	6.19	5.22	*−15.67*	1.42
Rhyolite green *facies*		74.9	72.38	*−3.36*	−2.16	−2.11	*−2.31*	5.9	5.37	*−8.98*	1.58
Rhyolite red *facies*		71.11	68.16	*−4.15*	7.08	5.59	*−21.05*	10.32	9.07	*−12.11*	3.53

Is to reproduce the experiment in real environment (practice of "test the test") by monitoring the same properties before and after the test.

Although the operation may take a long time, Δof some physical–mechanical parameters can be detect on stone materials already in exercise on a building for 18 years. In a similar case, it is possible to measure the "post-test" properties directly on building and the "pre-test" properties could be considered those of the same material in the quarry of origin.

CRediT authorship contribution statement

Fabio Sitzia: Conceptualization, Data curation, Formal analysis, Investigation, Project administration, Resources, Software, Supervision, Validation, Visualization, Writing - original draft, Writing-review and editing. **Carla Lisci:** Funding acquisition, Methodology, Validation, Visualization, Writing- review and editing. **José Mirão:** Funding acquisition, Investigation, Methodology, Validation, Visualization, Writing- review and editing.

Declaration of Competing Interest

The authors declare that they have no known competing financial interests or personal relationships that could have appeared to influence the work reported in this paper.

Acknowledgements

Fabio Sitzia gratefully acknowledges Sardinian Regional Government for the financial support of his PhD scholarship (P.O.R. Sardegna F.S.E. – Operational Programme of the Autonomous Region of Sardinia, European Social Fund 2014-2020 – Axis III Education and training, Thematic goal 10, Investment Priority 10ii), Specific goal 10.5.

The authors gratefully acknowledge the following funding sources: ColourStone—Colour of commercial marbles and limestone: causes and changings (ALT20-03-0145-FEDER-000017) and INOVSTONE4.0 (POCI-01-0247-FEDER-024535), co-financed by the European Union through the European Regional Development Fund (FEDER) and Fundação para a Ciência e Tecnologia (FCT) under the project UID/Multi/04449/2013 (POCI-01-0145-FEDER-007649).

References

[1] E. Strofer, Experimental measurement: interpreting extrapolation and prediction by accelerated aging, Restaurator 11 (1990) 254–266, https://doi.org/10.1515/rest.1990.11.4.254.
[2] X. Zou, T. Uesaka, N. Gurnagul, Prediction of paper permanence by accelerated aging I. Kinetic analysis of the aging process, Cellulose 3 (1) (1996) 243–267.
[3] H. Bansa, Accelerated aging tests in conservation research: Some ideas for a future method, Restaurator 13 (3) (1992) 114–137, https://doi.org/10.1515/rest.1992.13.3.114.
[4] P.L. Bégin, E. Kaminska, Thermal accelerated ageing test method development, Restaurator 23 (2002) 89–105, https://doi.org/10.1515/REST.2002.89.
[5] O.M. El-Feky, E.A. Hassan, S.M. Fadel, M.L. Hassan, Use of ZnO nanoparticles for protecting oil paintings on paper support against dirt, fungal attack, and UV aging, J. Cult. Heritage 15 (2) (2014) 165–172.
[6] H. Bansa, Accelerated aging of paper: some ideas on its practical benefit, Restaurator 23 (2002) 106–117, https://doi.org/10.1515/REST.2002.106.
[7] M. Credwson, Outdoor weathering must verify accelerated testing, Surf. Coat. Int. 91 (2008).
[8] R. Batterham, R. Rai, A comparison of artificial ageing with 27 years of natural ageing. AICCM. AICCM Book, Paper and Photographic Materials Symposium (2008).
[9] M.H. Ghobadi, R. Babazadeh, Experimental studies on the effects of cyclic freezing–thawing, salt crystallization, and thermal shock on the physical and mechanical characteristics of selected sandstones, Rock Mech. Rock Eng. 48 (3) (2015) 1001–1016.
[10] M. Mutluturk, R. Altindag, G. TurK, A decay function model for the integrity lost of rock when subjected to recurrent cycles of freezing–thawing and heating–cooling, Rock Mech. Min. Sci. 41 (2) (2004) 237–244, https://doi.org/10.1016/S1365-1609(03)00095-9.
[11] Giovanna Fioretti, Paolo Mazzoleni, Pasquale Acquafredda, Gioacchino Francesco Andriani, On the technical properties of the Carovigno stone from Apulia (Italy): physical characterization and decay effects by means of experimental ageing tests, Environ. Earth Sci. 77 (2) (2018), https://doi.org/10.1007/s12665-017-7201-9.
[12] G. Fioretti, Ageing test e analisi di degrado di rocce carbonatiche pugliesi impiegate come pietre ornamentali e da costruzione. PhD thesis. Politecnico di Bari (2016).
[13] ASTM D5312:2013. Standard Test Method for Evaluation of Durability of Rock for Erosion Control Under Freezing and Thawing Conditions.
[14] E. Molina, G. Cultrone, E. Sebastián, F.J. Alonso, Evaluation of stone durability using a combination of ultrasound, mechanical and accelerated aging tests, J. Geophys. Eng. 10 (3) (2013) 035003, https://doi.org/10.1088/1742-2132/10/3/035003.
[15] F. Fernandez, S. Germinario, (2017) Alteration and deterioration of natural stone materials: artificial aging as a tool of knowledge. Conference: VIIIth Conference "Diagnosis, Conservation and Valorization of Cultural Heritage" 14/15 December 2017.
[16] C. Thomachot, D. Jeannette, Evolution of the petrophysical properties of two types of Alsatian sandstone subjected to simulated freeze-thaw conditions, Geol. Soc. Lon. Spec. Publ. 205 (1) (2002) 19–32.
[17] UNI EN 14006:2013. Natural stone test methods - Determination of resistance to ageing by thermal shock.
[18] Mokhfi Takarli, William Prince, Rafat Siddique, Damage in granite under heating/cooling cycles and water freeze–thaw condition, Int. J. Rock Mech. Min. Sci. 45 (7) (2008) 1164–1175.
[19] M.F. Oliveira (2006) Ageing tests for dimension stone - experimental studies of granitic rocks from Brazil. Conference: IAEG2006, 10th Congress of the International Association for Engineering Geology and the Environment.
[20] Didem Eren Sarıcı, Thermal deterioration of marbles: Gloss, color changes, Constr. Build. Mater. 102 (2016) 416–421.
[21] UNI EN 12370:2001. Natural stone test methods - Determination of resistance to salt crystallisation.
[22] M. La Russa, S. Ruffolo, S. Belfiore, C. Aloise, P. Randazzo, R. Natalia, A. Pezzino, M. Giuseppe, Study of the effects of salt crystallization on degradation of limestone rocks, Periodico Mineral. 82 (2013) 113–127, https://doi.org/10.2451/2013PM0007.
[23] R. Přikryl, T. Lokajíček, J. Svobodová, Z. Weishauptová, Experimental weathering of marlstone from Přední Kopanina (Czech Republic)-historical building stone of Prague, Build. Environ. (2003), https://doi.org/10.1016/S0360-1323(03)00073-8.

[24] P. López-Arce, M.J. Varas-Muriel, B. Fernández-Revuelta, M. Álvarez de Buergo, R. Fort, C. Pérez-Soba, Artificial weathering of Spanish granites subjected to salt crystallization tests: surface roughness quantification, CATENA 83 (2-3) (2010) 170–185.
[25] UNI EN 13919:2004 Natural stone test methods - Determination of resistance to ageing by SO2 action in the presence of humidity.
[26] S. Gibeaux, C. Thomachot-Schneider, S. Eyssautier-Chuine, B. Marin, P. Vazquez, Simulation of acid weathering on natural and artificial building stones according to the current atmospheric SO_2/NO x rate, Environ. Earth Sci. 77 (9) (2018), https://doi.org/10.1007/s12665-018-7467-6.
[27] Soizic Gibeaux, Patricia Vázquez, Tim De Kock, Veerle Cnudde, Céline Thomachot-Schneider, Weathering assessment under X-ray tomography of building stones exposed to acid atmospheres at current pollution rate, Constr. Build. Mater. 168 (2018) 187–198.
[28] Bogdana Simionescu, Mihaela Olaru, Magda Aflori, Florica Doroftei, Siloxane-based polymers as protective coatings against SO 2 dry deposition, High Perform. Polym. 23 (4) (2011) 326–334.
[29] DIN 50018:1997. Sulphur dioxide corrosion testing in a saturated atmosphere.
[30] G. Cultrone, M.J. De La Torre, E.M. Sebastian, O. Cazalla, C. Rodriguez-Navarro, 2000. Behavior of brick samples in aggressive environments. Water. Air. Soil Pollut. (2000) https://doi.org/10.1023/a:1005142612180
[31] A.L. Velosa, M.R. Veiga, Development of artificial ageing tests for renders - Application to conservation mortars. In: Tompson G. (ed), Proceeding of 7th International Masonry Conference (2006).
[32] A. Arizzi, H. Viles, G. Cultrone, Experimental testing of the durability of lime-based mortars used for rendering historic buildings, Constr. Build. Mater. 28 (1) (2012) 807–818.
[33] R. Geiger, Classificação climática de Köppen-Geiger, Creat, Commons Attrib. Alike 3.0 Unported. (1936).
[34] M. Parry, H. Critchfield, General Climatology, Geogr. J. (1966). https://doi.org/10.2307/1792587.
[35] J.G. Lockwood, Danuta Martyn, Climates of the World, Geograph. J. 161 (3) (1995) 332, https://doi.org/10.2307/3059845.
[36] M. Pinna, L'atmosfera e il clima, Utet, Torino, 1978.
[37] F. Fulvi, Dizionario di geografia fisica, Newton Compton Roma. (1996).
[38] Louis C. Peltier, The geographic cycle in periglacial regions as it is related to climatic geomorphology, Ann. Assoc. Am. Geogr. 40 (3) (1950) 214–236.
[39] P.A. Warke, J.M. Curran, A.V. Turkington, B.J. Smith, Condition assessment for building stone conservation: a staging system approach, Build. Environ. 38 (9-10) (2003) 1113–1123.
[40] Bjørn Petter Jelle, Accelerated climate ageing of building materials, components and structures in the laboratory, J. Mater. Sci. 47 (18) (2012) 6475–6496.
[41] Ioanna Papayianni, Vasiliki Pachta, Maria Stefanidou, Analysis of ancient mortars and design of compatible repair mortars: the case study of Odeion of the archaeological site of Dion, Constr. Build. Mater. 40 (2013) 84–92.
[42] S. Aze, J.M. Vallet, M. Pomey, A. Baronnet, O. Grauby, Red lead darkening in wall paintings: Natural ageing of experimental wall paintings versus artificial ageing tests, Eur. J. Mineral. 19 (2013) 883–890, https://doi.org/10.1127/0935-1221/2007/0019-1771.
[43] G. Pavlendová, R. Podoba, I. Baník, Accelerated ageing in testing bricks used in the conservation of historic buildings, in: AIP Conference Proceedings. https://doi.org/10.1063/1.4903026.
[44] Barun Shankar Gupta, Bjørn Petter Jelle, Tao Gao, Wood facade materials ageing analysis by FTIR spectroscopy, Proc. Inst. Civil Eng. Constr. Mater. 168 (5) (2015) 219–231.
[45] Dennis Kronlund, Mika Lindén, Jan-Henrik Smått, A polydimethylsiloxane coating to minimize weathering effects on granite, Constr. Build. Mater. 124 (2016) 1051–1058.
[46] Mauro F. La Russa, Natalia Rovella, Monica Alvarez de Buergo, Cristina M. Belfiore, Antonino Pezzino, Gino M. Crisci, Silvestro A. Ruffolo, Nano-TiO2 coatings for cultural heritage protection: the role of the binder on hydrophobic and self-cleaning efficacy, Prog. Org. Coat. 91 (2016) 1–8.
[47] Enrico Sassoni, Gabriela Graziani, Elisa Franzoni, George W. Scherer, New method for controllable accelerated aging of marble: Use for testing of consolidants, J. Am. Ceram. Soc. 101 (9) (2018) 4146–4157.
[48] A. Zornoza-Indart, P. López-Arce, J. Simão, N. Leal, K. Zoghlami, Accelerated aging experiments with saline fog, involving ventilation in calcarenitic monument rocks, Comun. Geol. 101 (3) (2014) 1181–1185.
[49] Maria Idália Gomes, Paulina Faria, Teresa Diaz Gonçalves, Rammed earth walls repair by earth-based mortars: the adequacy to assess effectiveness, Constr. Build. Mater. 205 (2019) 213–231.
[50] P. López-Arce, M. Tagnit-Hammou, B. Menéndez, J-D. Mertz, A. Kaci, Durability of stone-repair mortars used in historic buildings from Paris, Mater. Struct. 49 (12) (2016) 5097–5115.
[51] Stefano Columbu, Carla Lisci, Fabio Sitzia, Giampaolo Buccellato, Physical–mechanical consolidation and protection of Miocenic limestone used on Mediterranean historical monuments: the case study of Pietra Cantone (southern Sardinia, Italy), Environ Earth Sci. 76 (4) (2017), https://doi.org/10.1007/s12665-017-6455-6.
[52] Marjorie Wilson, Hilary Downes, Tertiary-Quaternary intra-plate magmatism in Europe and its relationship to mantle dynamics, Geol. Soc. Lond. Memoirs 32 (1) (2006) 147–166.
[53] G. Forestieri, A. Tedesco, M. Ponte, Olivito, R, Local building stones used in Calabrian architecture: calcarenite and sandstone of the Tyrrhenian Coastal Range of Cosenza Province (Italy). Conference: Le vie dei Mercanti – XIV International Forum. World Heritage and degradation (2016)
[54] P. Primavori, Carrara Marble: a nomination for 'Global Heritage Stone Resource' from Italy, Geol. Soc. Lond. Spec. Publ. 407 (1) (2015) 137–154.
[55] Sema Yurtmen, George Rowbotham, Fikret İşler, Peter A. Floyd, Petrogenesis of Basalts from Southern Turkey: the Plio-Quaternary Volcanism to the North of İskenderun Gulf, Geol. Soc. Lond. Spec. Publ. 173 (1) (2000) 489–512.
[56] A. Peccerillo, Plio-Quaternary Volcanism in Italy, Petrology Geochemistry, Geodynamics, Springer, Heidelberg, 2005.
[57] T. Engidasew, Engineering Geological Characterization of Volcanic rocks of Ethiopian and Sardinian (Italy) highlands to be used as construction materials PhD thesis, University of Cagliari, 2018.
[58] S. Columbu, F. Antonelli, F. Sitzia, Origin of Roman worked stones from St. Saturnino Christian Basilica (south Sardinia, italy), Mediterranean J. Archeaol. Archaeom. 18 (5) (2018) 17–36, https://doi.org/10.5281/zenodo.1256047.
[59] F. Sitzia, Decay Monitoring and Conservation of Sardinia Monumental Heritage Through Geochemical, Petro-Physical and Micro-Photogrammetric Characterization of Stone Surfaces PhD thesis, University of Cagliari, 2019.
[60] Stefano Columbu, Petrographic and geochemical investigations on the volcanic rocks used in the Punic-Roman archaeological site of Nora (Sardinia, Italy), Environ. Earth Sci. 77 (16) (2018), https://doi.org/10.1007/s12665-018-7744-4.
[61] A. Pala, Carta Idrogeologica di Cagliari, Coedisar, Cagliari, 1997.
[62] P.B. Serra, P. Bacco, Forum Traiani: il contesto termale e l'indagine archeologica di scavo, L'Africa romana 7 (1998) 1213–1255.
[63] Sitzia Fabio, Beltrame Massimo, Columbu Stefano, Lisci Carla, Miguel Catarina, Mirão José, Ancient restoration and production technologies of Roman mortars from monuments placed in hydrogeological risk areas: a case study, Archaeol. Anthropol. Sci. 12 (7) (2020), https://doi.org/10.1007/s12520-020-01080-8.
[64] http://clima.meteoam.it/AtlanteClimatico.
[65] https://giovanni.gsfc.nasa.gov/giovanni.
[66] UNI EN 12407:2019 Natural stone test methods-petrographic examination
[67] Chester K. Wentworth, A scale of grade and class terms for clastic sediments, J. Geol. 30 (5) (1922) 377–392.
[68] S. Columbu, M. Palomba, F. Sitzia, M.R. Murgia, Geochemical, mineral-petrographic and physical-mechanical characterization of stones and mortars from the Romanesque Saccargia Basilica (Sardinia, Italy) to understand their origin and alteration, Italian, J. Geosci. 137 (3) (2018) 369–395, https://doi.org/10.3301/IJG.2018.04.
[69] UNI EN 1936:2007 Natural stone test methods-determination of real density and apparent density, and of total and open porosity.
[70] UNI EN 14617-1:2013 Agglomerated stone, test methods-part 1: determination of apparent density and water absorption.
[71] ISRM 1985: International society for rock mechanics commission on testing methods: suggested method for determining point load strength.
[72] A. Palmström, RMi – A Rock Mass Characterization System for Rock Engineering Purposes PhD thesis, University of Oslo, 1995.
[73] S. Gaurav, Digital Color Imaging Handbook (1.7.2 ed.), CRC Press. (2003).
[74] AM, Aeronautica militare Italiana, La radiazione solare globale e la durata del soleggiamento in Italia dal 1991 al 2010
[75] ASTM D3424-11, Standard Practice for Evaluating the Relative Lightfastness and Weatherability of Printed Matter (Withdrawn 2020).
[76] G. Pecorini, Su un deposito lacustre oligocenico della Nurra di Alghero, Atti Acc. Naz. Lincei, Rend. Cl. Sc. Fis. Mat. e Nat. 30 (1961) 67-73.
[77] A. Cherchi, Appunti biostratigrafici sul Miocene della Sardegna (Italia), Mem. B.R.G.M. 78 (1974) 433–445.
[78] Stefano Columbu, Anna Gioncada, Marco Lezzerini, Fabio Sitzia, Mineralogical-chemical Alteration and Origin of Ignimbritic Stones Used in the Old Cathedral of Nostra Signora di Castro (Sardinia, Italy), Stud. Conserv. 64 (7) (2019) 397–422.
[79] S. Columbu, M. Palomba, F. Sitzia, G. Carcangiu, P. Meloni, Pyroclastic Stones as Building Materials in Medieval Romanesque Architecture of Sardinia (Italy): Chemical-Physical Features of Rocks and Associated Alterations. International Journal Of Architectural Heritage. https://doi.org/10.1080/15583058.2020.1749729.
[80] Noushine Shahidzadeh-Bonn, Julie Desarnaud, François Bertrand, Xavier Chateau, Daniel Bonn, Damage in porous media due to salt crystallization, Phys. Rev. E 81 (6) (2010), https://doi.org/10.1103/PhysRevE.81.066110.
[81] Michael Steiger, Crystal growth in porous materials—I: The crystallization pressure of large crystals, J. Cryst. Growth 282 (3-4) (2005) 455–469.
[82] P. Aloise, L. Randazzo, N. Rovella, A. Pezzino, G. Montana, Study of the effects of salt crystallization on degradation of limestone rocks, Periodico di Mineralogia 82 (1) (2013) 113–127.
[83] H. De Clercq, The effect of other salts on the crystallisation damage to stone caused by sodium sulphate. In: L. Ottosen (ed) SWBSS 2008, Proceedings of the 1st international conference on salt weathering of buildings and stone sculptures, Copenhagen, pp 307–315.
[84] T. Godish, Indoor Environmental Quality, CRC Press, 2001.
[85] ICOMOS-ISCS, Illustrated glossary on stone deterioration patterns
[86] B.J. Smith, A. Török, J.J. McAlister, Y. Megarry, Observations on the factors influencing stability of building stones following contour scaling: a case study of oolitic limestones from Budapest, Hungary, Build. Environ. 38 (9-10) (2003) 1173–1183.
[87] Barbara Lubelli, Veerle Cnudde, Teresa Diaz-Goncalves, Elisa Franzoni, Rob P.J. van Hees, Ioannis Ioannou, Beatriz Menendez, Cristiana Nunes, Heiner Siedel, Maria Stefanidou, Veronique Verges-Belmin, Heather Viles, Towards a more

effective and reliable salt crystallization test for porous building materials: state of the art, Mater. Struct. 51 (2) (2018), https://doi.org/10.1617/s11527-018-1180-5.
[88] J.D. Rodriguez, Stone patina. A controversial concept of relevant importance in conservation, In: proceedings of International Seminar Theory and Practice in Conservation. A tribute to Cesare Brandi (2006) Lisbon, Portugal.
[89] P. Tiano, C. Pardini, Le patine, genesi significato e conservazione. ICV, (2004).
[90] Elisa Franzoni, Enrico Sassoni, George W. Scherer, Sonia Naidu, Artificial weathering of stone by heating, J. Cult. Heritage 14 (3) (2013) e85–e93.
[91] Quansheng Liu, Shibing Huang, Yongshui Kang, Xuewei Liu, A prediction model for uniaxial compressive strength of deteriorated rocks due to freeze–thaw, Cold Reg. Sci. Technol. 120 (2015) 96–107.
[92] Gholamreza Khanlari, Yasin Abdilor, Influence of wet–dry, freeze–thaw, and heat–cool cycles on the physical and mechanical properties of Upper Red sandstones in central Iran, Bull. Eng. Geol. Environ. 74 (4) (2015) 1287–1300.
[93] A. Pellegrino, Proprietà geotecniche dei materiali a grana grossa, Geotecnica (1965).
[94] A. Lo Monaco, M. Marabelli, C. Pelosi, M. Salvo, Colour measurements of surfaces to evaluate the restoration materials. In: Proceedings of SPIE – The International Society for Optical Engineering 8084, Volume: 8084 (2011).
[95] Nicola Careddu, Graziella Marras, The effects of solar UV radiation on the gloss values of polished stone surfaces, Constr. Build. Mater. 49 (2013) 828–834.
[96] E.M. Winkler Stone in architecture: properties, durability, 3rd edn. Springer, Berlin (1997). https://doi.org/10.1007/978-3-662-10070-7.
[97] J.A. Harrell, M.A.T.M. Broekmans, D.I. Godfrey-Smith, The origin, destruction and restoration of colour in Egyptian travertine, Archaeom 49 (2007) 421–436, https://doi.org/10.1111/j.1475-4754.2007.00312.x.
[98] Rafael Navarro, Lidia Catarino, Dolores Pereira, Francisco Paulo de Sá Campos Gil, Effect of UV radiation on chromatic parameters in serpentinites used as dimension stones, Bull. Eng. Geol. Environ. 78 (7) (2019) 5345–5355.
[99] M. O'Donoghue, Gems, Sixth edition., Butterworth-Heinemann, 2006.
[100] T.C. Meierding, Weathering of serpentine stone buildings in the Philadelphia region: a geographic approach related to acidic depo- sition. In: Turkington AV (ed) Stone decay in the architectural envi- ronment. Geol Soc Lond Spec Publ 399 (2005) 17–25.
[101] R.F. Witzel, R.W. Burnham, J.W. Onley, Threshold and suprathreshold perceptual color differences, J. Opt. Soc. Am. 63 (5) (1973) 615, https://doi.org/10.1364/JOSA.63.000615.